USE OF HIGH-RESOLUTION SIDESCAN SONAR DATA TO QUANTITATIVELY MAP AND MONITOR A MID-CONTINENTAL SHELF HARBOTTOM: 23-MILE SITE, ONSLOW BAY, NC

Matthew Edward Head

A Thesis Submitted to the
University of North Carolina at Wilmington in Partial Fulfillment
Of the Requirements for the Degree of
Master of Science

Department of Earth Sciences

University of North Carolina at Wilmington

2004

Approved by

Advisory Committee

_____ _____

_____
Chair

Accepted by

_____
Dean, Graduate School

This thesis has been prepared in a style and format

consistent with

Continental Shelf Research

TABLE OF CONTENTS

ABSTRACT

This study attempts to constrain the spatial and temporal variations in the seafloor morphology, as well as the relationship between sidescan sonar data and seafloor characteristics at the 23-Mile hardbottom area on the mid-continental shelf of Onslow Bay, NC. The 23-Mile site consists of an upper limestone hardbottom at 29-30m water depth covered in a thin discontinuous veneer of sediments. The lower sand flats at 32-33m depth consist of concentrated areas of contrasting grain size. A dual-frequency sidescan sonar system was used to repeatedly image the seafloor of a 3.5 km by 2.1 km region at 23-mile site over a period of 2.5 years. Cruises were conducted in December 1999, December 2000, July 2001, and May 2002. Textural analysis of the sidescan sonar imagery was conducted using gray-level co-occurrence matrices. Two textural indices: entropy (acoustic roughness), and homogeneity (level of textural organization) were used in conjunction with gray-level to identify seabed types. The textural analysis successfully identified three of the four chosen seabed types. Groundtruthing by divers indicates that these units show a strong statistical correlation between backscatter intensity and sediment grain size. Subsurface scattering also appears to play a role in the backscatter intensity. A comparison of results between successive surveys shows a significant difference in the spatial orientation of the coarse-grained and fine-grained contacts of the lower sand flats. Significant displacements (>10m) and changes in morphology of contacts in five study areas suggest that the fine-grain sands in this area are highly mobile. The first observation period (1999-2000) represents an entire year of movement, which resulted in a consistent shift in the south to southeast direction in all of the areas except for one. The second observation period (2000-2001) comprised the

winter and spring seasons. The contact movement displayed a consistent shift to the north-northwest in all study areas except two. Individual events (nor'easters and fair-weather) identified from the near-bottom measurements of waves and currents provide mechanisms for the observed sand movement seen in the sidescan surveys.

ACKNOWLEDGEMENTS

I would first and foremost like to thank my academic advisor, Dr. Nancy R. Grindlay, without her patience and enthusiasm this project would not have been possible. I would also like to thank the members of my advisory committee, Dr. Lynn Leonard and Dr. Martin Posey, whose insight and feedback have made this project a success. The entire Coastal Marine Geophysics Laboratory has made this entire process an enjoyable one. Ansley Wren and Susan Blake of the Coastal Sediments Lab were indispensable in this study.

I would also like to thank Capt. Dan Aspenleiter, Capt. Gerry Compeau and the crews of the R/V Cape Fear, and the R/V Seahawk. Sharon Kissling, Jay Souza, David Wells, Susie Holst, John Murray, and Randy Turner were instrumental in the diving and sidescan sonar operations. Funding for this project was provided by NOAA/OAR grants. I would also like to thank the UNCW Graduate School and Department of Earth Sciences, and the Geological Society of America for financial support of my research and studies.

Special thanks go to Dr. Walter Martin of the University of North Carolina at Charlotte for his tireless devotion to his students. He has influenced my future more than he will ever know. Without his motivation I would not have pursued a higher education.

DEDICATION

I would like to dedicate this work to my family and friends. Each and every one of you has not only made this possible, but enjoyable as well. To my parents and sister, thank you so much for the emotional and financial support. You are the very reason that I am where I am today. Lastly, I would like to dedicate this to Michael Sanborn Sheldt. May you enjoy all that Heaven has to offer. Aloha little brother.

LIST OF TABLES

Table Page

LIST OF FIGURES

Figures Page

INTRODUCTION

Onslow Bay is a sediment-starved and ecologically productive system on the southeastern North Carolina continental margin. It is bordered to the north by Cape Lookout, to the east by the continental shelf break, to the south by Cape Fear, and to the west by the shoreface (Fig 1). The inner to middle continental shelf of Onslow Bay is characterized by a complex sequence of rocky outcrops with relief of up to 10m (Riggs et al., 1996, 1998). Surficial sediments are scattered throughout the bay in a thin discontinuous veneer. Aside from the authigenic carbonate component, most of the surficial sediment is relict; it derives from the erosion and reworking of outcropping pre-Holocene strata (Riggs et al., 1996, 1998). The sediment distribution and composition is complicated by extensive Pleistocene infilled channels, and topographic hardbottoms of various compositions (Riggs et al., 1996, 1998). These hardbottoms provide important habitats for a diverse community of benthic organisms that form the framework for highly productive "livebottom" communities (Renaud et al., 1996, 1997; Riggs et al., 1998). Significant storm events (hurricanes and nor'easters) are suspected to modify the sediment structures of the hardbottoms, and the distribution of the associated benthic communities (Renaud et al., 1996, 1997; Riggs et al., 1998; Posey and Ambrose, 1994).

Continued study of Onslow Bay is needed to identify additional hardbottom areas, and to understand and quantify the impacts of sediment mobility on these regions important to both commercial and recreational fisheries. While most seabed assemblages and resources can only be sampled and monitored directly using diver observations or other large-scale (>1:10,000) survey techniques, it is impractical to apply this level of

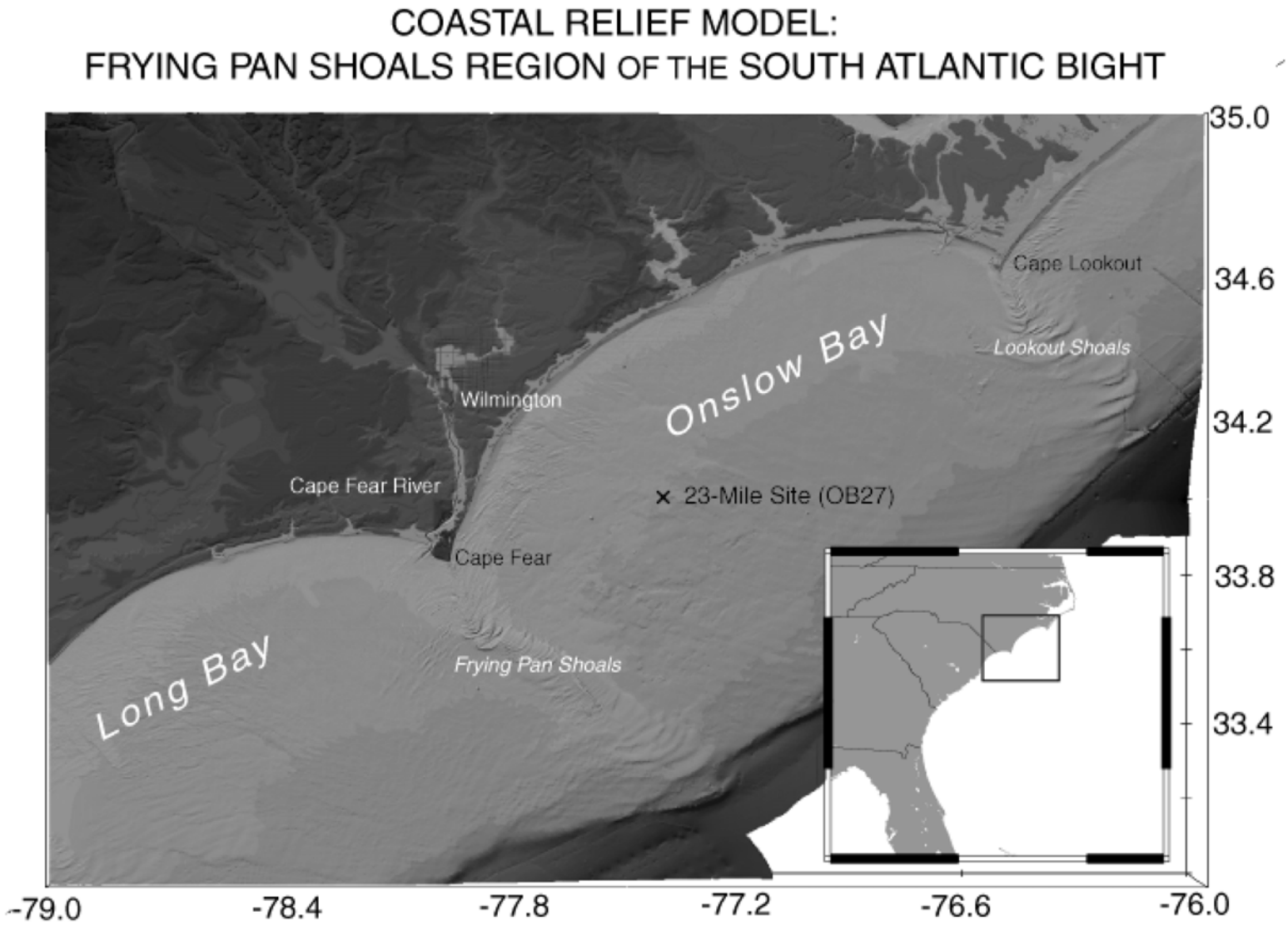

Figure 1: Coastal relief model for Onslow Bay. This model is constructed from National Geophysical Data Center (NGDC) bathymetry at a 3-arc-second grid interval.

effort to the entire southeastern Atlantic continental shelf. There is a need, therefore, to establish a cost-effective means of remotely (e.g. shipboard) identifying the location of hardbottoms and to measure temporal variations of seabed morphology and sedimentary properties. This study will evaluate the utility of high-resolution sidescan sonar in mapping and monitoring seabed habitats at a known hardbottom site, 23-mile reef site, in Onslow Bay, NC.

The research questions that will be addressed in this study include the following:

1. What is the relationship between seabed types that are to a large extent controlled by sedimentary properties (e.g. grain size, sorting, mineralogy), sedimentary structures, and observations, and interpretations of remotely sensed acoustic data? Can this relationship be modeled or quantified?

2. How have the seabed habitats at 23-mile site changed their characteristics and spatial distribution between 12/1999 and 04/2002?

BACKGROUND

The ultimate goal of sidescan sonar mapping is a quantitative interpretation of the seafloor properties (e.g. grain size, composition, bed roughness). The acoustic backscatter response recorded by sidescan sonar systems is well suited for the detection of sediment cover contrasts on the seafloor, because to a large extent it appears that spatial trends in backscatter correspond to changes in texture and microtopography of the sediments (Johnson and Helferty, 1990; LeBlanc et al., 1992 & 1995). Numerous researchers have undertaken the study of the acoustic properties of sediments to establish relationships between backscatter response and sediment characteristics, in order to

interpret remotely sensed data (e.g. Blondel et al., 1993 & 1998; LeBlanc et al., 1995; Ryan and Flood, 1996; Goff 2000; Cochrane & Lafferty 2002).

Parameters Controlling Acoustic Backscatter Strength

Grain Size

Several studies have noted the importance of sediment grain size to the sidescan sonar acoustic backscatter (Ryan and Flood, 1996; Goff 1999, 2000; LeBlanc et al., 1995; Davis et al., 1996). Sonar images result from seafloor topography and the acoustic properties of the sediments. Grain size is intrinsic to each of these components. The size of the grain is directly related to the microtopography of the seafloor. A rougher bottom will scatter more of the acoustic pulse. Therefore, the greater the grain size, the greater the scattering of the acoustic signal. Davis et al. (1996) and Leblanc et al. (1995) quantitatively examined the first-order relationships between surficial sediment properties and sidescan sonar response. The results of these studies suggested that sediment grain size was the dominant controlling variable on the backscatter strength. Goff et al. (2000) examined the dependence of acoustic backscatter variations on sediment grain-size distribution by correlating 95kHz sidescan data with approximately 300 grab samples on the New Jersey shelf. The relationship showed a positive linear correlation, but the application was limited because the data were primarily grouped in the finer sediment sizes and lower signal strengths. The coarser, higher energy sediment samples did not fit the trend line as well. Those samples that contained a wide range of grain sizes, consistently showed high-energy backscatter, indicating that a few large-grain particles may dominate the acoustic characteristics of a sediment sample.

Carbonate Composition

Davis et al. (1996) also found a relationship between backscatter and the carbonate composition. This study showed that backscatter increased with increasing grain size and percent carbonate composition. This relationship does not appear to be a function of the acoustic properties of the $CaCO_3$, and rather is mostly likely related to the size and shape of these particles. There are two possible reasons for the relationship: (1) the increase in carbonate composition results in an increase in the mean grain size, and (2) the shape of the carbonate fragments (typically shell fragments) that tend to be flat with many angles. The flat-lying shell fragments are more effective at backscattering acoustic energy than a spheroidal sand grain.

Subsurface Scattering

Ryan and Flood (1996) studied sonar backscatter response at dual frequencies. Their study showed that dual frequency systems have the ability to distinguish subsurface scatterers from seabed textural features. This is possible due to differences in attenuation of the dual frequencies. A 30/72 kHz system and a 100/500 kHz system were used. Each of these systems was able to profile the subsurface, with the 30/72 kHz system having the greatest degree of subsurface penetration. The 100/500 kHz system was effective in imaging surface, and near-surface scattering features. The 100 kHz frequency signal was able to penetrate the softer sediments with no internal volume scatterers (e.g. homogenous body of mud or silt). The 500 kHz frequency signal, however, was unable to effectively penetrate the surface. In comparing the resultant 100 and 500 kHz mosaics, it was possible to discern the relative contribution of surficial reflectors from the subsurface reflectors in the overall returned signal. The 30/72 kHz system was able to

discriminate the sub-bottom scatterers from the seabed textural features revealing buried hardbottom containing karst-like depressions (Ryan and Flood, 1996).

Biota

Few studies have addressed how the benthic biota may affect the backscatter signal. Brown et al. (2002) attempted to use sidescan sonar to map various benthic habitats in the English Channel. The study site was divided into distinct acoustic regions identified by the strength of the return. Underwater video footage established that differences between the acoustic regions were due to changes in substrate type, and that substrates were generally homogenous within each of the regions (Brown et al., 2002). Grab samples were then taken in the different areas to ground-truth the biota and sediment characteristics seen in the video and sonographs. The analysis revealed several biological assemblages (e.g. echinoderm-dominated, gravelly sand with occasional sand veneers) corresponded to distinct backscatter patterns when imaged with high-resolution sidescan sonar.

In summary, there appears to be a strong positive correlation between grain-size and acoustic backscatter strength. However, other factors also influence the backscatter response such as percent carbonate composition, subsurface scattering, and possibly benthic biota.

Seabed Classification Using Sidescan Sonar Imagery

Spectral Parameters of Sidescan Sonar Imagery

Most of the acoustic energy arriving on the seafloor is scattered forward in the specular direction away from the sidescan sonar system. A small portion is lost in the

sediments, and a small portion (several orders of magnitude smaller than the incident wave) is scattered back to the sonar, amplified and recorded (Blondel and Murton, 1997). This received signal is then given values based upon the relative strength of the return. The returns are assigned a gray level value for each pixel (0-255). It is these values, when displayed and georeferenced that field the sidescan sonar mosaic. These gray-level values denote the spectral parameters of the imagery, and allow for a quantitative analysis of the imagery for seafloor classification.

Textural Analysis of Sidescan Sonar Imagery

The mere use of gray levels to classify the seabed has proven inadequate, because sidescan sonar imagery is often stretched to non-uniform background backscatter values during processing (Blondel et al., 1996). Textural parameters, a description of the spatial organization of levels-levels within a small computational window, however, have promise for use in seabed classification (Haralick et al., 1973). Grey level co-occurrence matrices (GLCMs), a second-order texture parameter, have been used successfully to characterize texture in various fields of remote sensing (e.g. Shokr, 1991; Blondel et al., 1993; Blondel and Murton, 1997; Blondel et al., 1998; Gao et al., 1998; Cochrane and Lafferty, 2002; Huvenne et al., 2002). The matrices are difficult to interpret themselves; instead they are reduced to a single statistical measure for each pixel, called a textural index (Haralick et al., 1973; Blondel and Murton, 1997). The GLCM entries are derived from the gray level of pixels located inside a small region within the image based on their relationship to adjacent pixels (Shokr, 1991; Blondel and Murton, 1997). Each entry into the matrix represents the occurrence of a possible pair of gray levels measured at two

pixels, which are separated by a given displacement vector (Haralick et al., 1973). It is assumed that the texture information is specified by values f_{ij} within the GLCM, where f_{ij} denotes the frequency of occurrence of two cells of gray-level i and j, with a distance d in a given direction, and $p(i,j)$ denotes the (i,j)th entry in a normalized GLCM.. Typically only four directions corresponding to 0^o, 45^o, 90^o, and 135^o are used (Tso and Mather, 2001). Below are the equations for homogeneity (IDM) and entropy:

$$\text{Homogeneity} = \sum_i \sum_j \frac{1}{1+(i-j)2} p(i,j)$$

$$\text{Entropy} = -\sum_i \sum_j p(i,j) \log p(i,j)$$

Statistical parameters can then be derived from the matrix to characterize texture (Shokr, 1991). Blondel (1996) found two indices, entropy and homogeneity (as defined by Shokr, 1991) to be particularly useful for analysis of sidescan sonar imagery in seabed classification. Entropy is a measure of the acoustic roughness, and homogeneity measures the level of textural organization (Blondel and Murton, 1997). Therefore, the lowest entropy values would correspond to lower bed roughness, and these values would increase as the roughness of the seafloor increased. Homogeneity is directly proportional to the amount of local similarities within the computational window.

STUDY AREA

Over the past fifteen years, 23-mile reef site has been the focus of intense geological and biological research (Mearns et al., 1988; Posey and Ambrose, 1994; Riggs

et al., 1996,1998; Renaud et al., 1998). The 23-mile site is characterized by a hardbottom, ledge complex. It can be subdivided into three distinct habitats: the upper flat hardbottom, the scarp and rubble ramp complex, and the lower sand flats (Fig 2)(as defined by Renaud et al., 1996 & 1997). These areas were classified mainly using diver observations such as video and sediment analysis.

Upper Flat Hardbottom

The upper flat hardbottom is a flat surface composed of a Pleistocene limestone shelf covered by a thin veneer (<30 cm) of mobile fine sands (Renaud et al., 1996; 1997). Scattered coral, sponges, and various other invertebrates project through the sands. Frequently, large expanses of hardbottom are cleared of sand, allowing for colonization of brown macroalgae and sessile invertebrates.

Scarp and Rubble Ramp Complex

The scarp and rubble ramp complexes are narrow, linear features that meander across the continental shelf. Due to the variability in the thickness and resistance to erosion, these ledges can exhibit an enormous variability in scarp geometry, exposed surface area, size of rubble blocks, and the extent of the rubble field (Riggs et al., 1996; 1998). The average vertical relief of the reef scarp at the 23 Mile site is 2-5m. The rubble blocks form as the Miocene mudstone is cut from beneath the limestone hardbottom until the structural integrity is compromised. The overlying Pleistocene limestone then falls to the sand below (Riggs et al., 1996). This zone is characterized by the greatest density of algal and invertebrate communities (Riggs et al., 1996, 1998). The delineation between

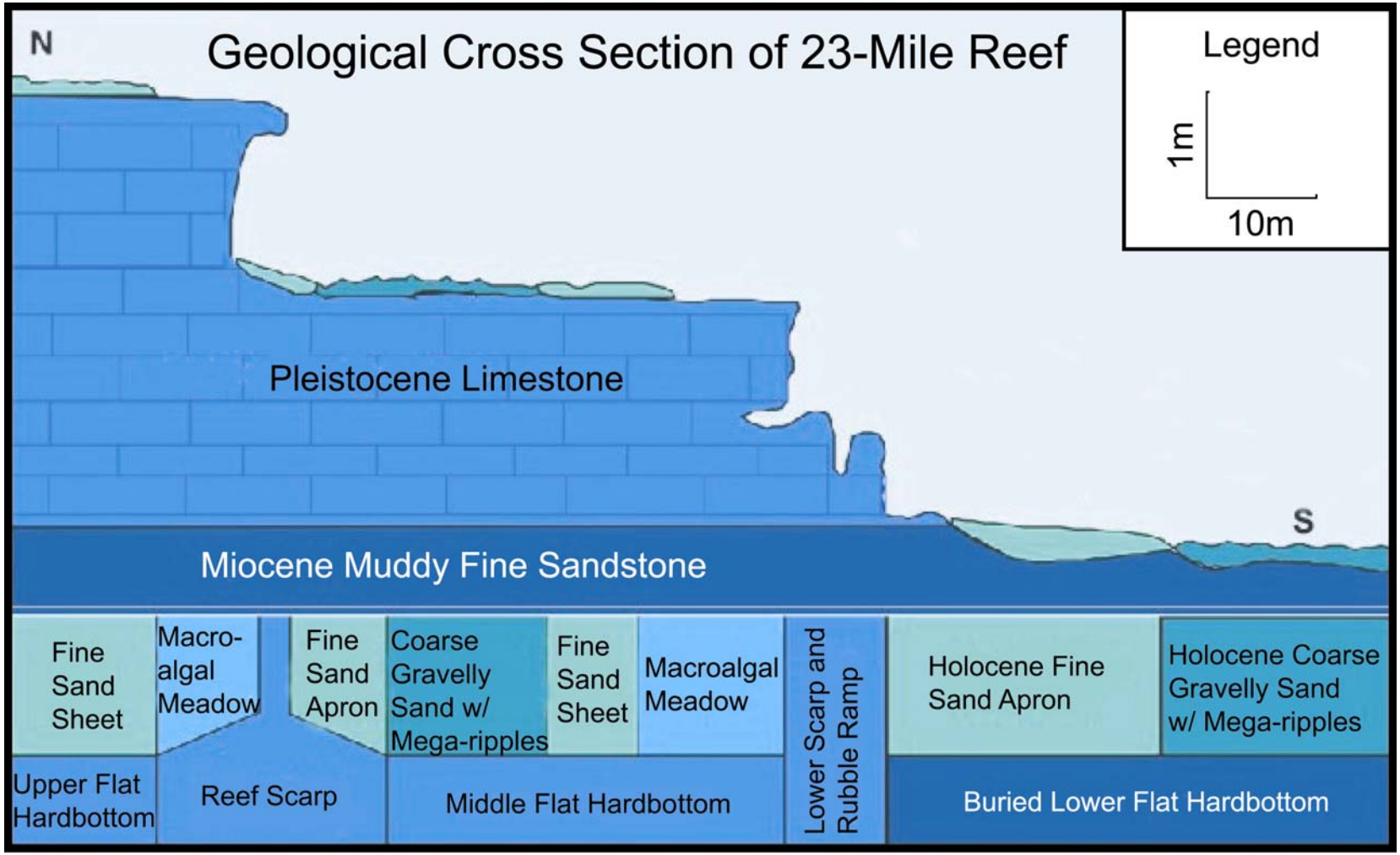

Figure 2: Geologic cross section for 23 Mile site. This profile was adapted from a profile published in Riggs et al., 1996 & 1998. For location of transect see Figure 5.

this zone and the lower sand flats is very distinct. The reef scarp and rubble ramp are subject to bioerosion and reworking, resulting in a coarse sand fraction.

Lower Sand Flat

The lower sand flat is characterized by sharp contrasts between fine sand bodies and mega-rippled, gravelly sand bodies. The coarse gravelly sands form a lag pavement in the topographic lows between erosional scarps on the shelf floor; they do not occur on the hardbottom surfaces (Riggs et al., 1996; 1998). Fine sands occur as extensive thin sheets overlying the gravelly sands throughout the lower sand flats (Riggs et al., 1996; 1998). The coarse gravelly sands often contain patches of microalgae with scattered clumps of brown macroalgae and some red algae attached to coarser pieces of shell and rock, while the fine sand aprons are nearly free of macroalgae and surface dwelling sessile invertebrates (Renaud et al., 1996; 1997).

Previous and On-going Monitoring Efforts at the Study Site

Several studies have looked at the effects of episodic storm events on Onslow Bay, and specifically the hardbottom reef complexes that exist there (Mearns et al., 1988; Renaud et al., 1996, 1997; Riggs et al., 1998). Mearns et al., (1988) examined the effects of Hurricane Diana (September 11-13, 1984; Category 3) on a hardbottom area on the mid-continental shelf of Onslow Bay, using repeat sidescan sonar surveys. Mearns et al. (1988) focused on the change of the reef scarp and rubble ramp. They failed to find any measurable differences between the pre- and post-storm sidescan imagery. The qualitative change detection analysis, however, was performed on imagery collected by two different sidescan systems with different resolution capabilities. While changes in

large-scale features (e.g. geometry of reef ledge) would be distinguishable between the two data sets, it is unlikely that small-scale changes (e.g. bedforms) would be detectable given the different resolutions.

Riggs et al. (1998) focused on the sediment production, storm dynamics, and the interrelationship between hardbottoms and sediment dynamics in four study areas including 23-Mile, and three other sites on the mid-continental shelf of Onslow Bay. The study focused on reef scarps and the immediately adjacent areas during short duration, episodic events from 1980 through 1995. Through the use of sediment traps and diver observations, Riggs et al. (1998) found that during significant storm events the entire fine sand sheet could be suspended, potentially settling and burying the rippled coarse gravelly sands and various hardbottom outcrops. Riggs et al. (1998) also found that the rippled gravelly sands were reactivated during extreme storm events. However, no information on the direction or magnitude of these sediment movements was offered.

Renaud et al. (1996 & 1997) focused on the effects of these storm events upon the benthic hardbottom communities in southwestern Onslow Bay including 23-Mile. They found that severe storms could have a profound effect on the distribution of marine sediments that could, in turn, influence the development of benthic communities (Renaud et al., 1996). Intense storms have the potential to create new benthic habitat (i.e. exposed hardbottom), especially suitable habitat for benthic macroalgae. It was also discovered that the mobilization of these sediments could cover exposed hardbottom, thereby making it unsuitable for colonization by sessile organisms (Posey et al., 1996).

More recently, an instrumented frame was deployed at 23-mile site (32 m water depth) as part of the NOAA-funded Coastal Ocean Research Monitoring Program

(CORMP). The instrumented frame, equipped with CT loggers, an Acoustic Doppler Current Profiler (ADCP), a Pulse Coherent-ADCP, and two optical backscatter sensors, has been recording temperature, salinity, water column turbidity, bottom elevation and current direction and velocity at 23-mile reef during the past 2.5 years. The data are collected continuously for four to six weeks (limited by battery life), when it is then necessary to remove the instruments for servicing and downloading of the data. They are then redeployed as soon as possible. Data collected by these instruments provide information about physical forcing mechanisms that can be used to link the observed changes in the spatial distribution of sedimentary features.

OBJECTIVES

The main objectives of this study are to:

1. Use sedimentological samples and sidescan sonar imagery to identify sedimentological/geological characteristics of the seafloor near 23 mile.

2. Develop a quantitative method to remotely map the seabed habits using high-resolution sidescan sonar data.

3. Determine the magnitude of spatial and temporal changes in sedimentary morphology and distribution within the study area, through repeat diver observations and sidescan sonar surveys over a 2.5-year period. The focus will be on the lower-sand flats habitat where changes in fine-grained and course-grained sand distributions will be examined.

DATA SETS

Sidescan Sonar Imagery

Four sidescan sonar cruises near the 23-mile site covering an area of 3.5 km by 2.1 km were conducted (Dec. 1999, Dec. 2000, June 2001, and April 2002). Sidescan sonar data were collected using the EdgeTech DF1000 dual frequency (100 kHz and 500 kHz) digital towfish. The data were collected aboard UNCW's 70' *R/V Cape Fear*.

The surveys consisted of nine sonographs (lines) collected at 100 kHz trending east to west in an area bounded by 34° 00' 11"N and 77° 22' 31"W in the northwest and 33° 59' 10"N and 77° 20' 18"W in the southeast (Fig. 3). Navigation for the georeferencing of the sidescan data was collected from a Nobeltec differential global positioning system (DGPS). The accuracy of the DGPS is $\pm$3-5m. In addition to this error, uncertainty in the location of the tow-fish must be accounted for, resulting in an overall error of $\pm$10m. These navigation data were routed directly into the acquisition system. Acquisition parameters were held constant in all surveys, except for the range in the 12/00 survey (Table 1). The range of 300m was twice that of the other surveys.

Processing of the sidescan sonar data was conducted using the TEI ISIS Sonar and DelphMap packages. Geometric and radiometric corrections were applied to the sonographs during processing (Appendix A). The sonographs were then mosaicked individually at a 0.25m by 0.25m pixel resolution, and were displayed in a reversed gray-scale of 0-255 and output into the TEI DelphMap program.

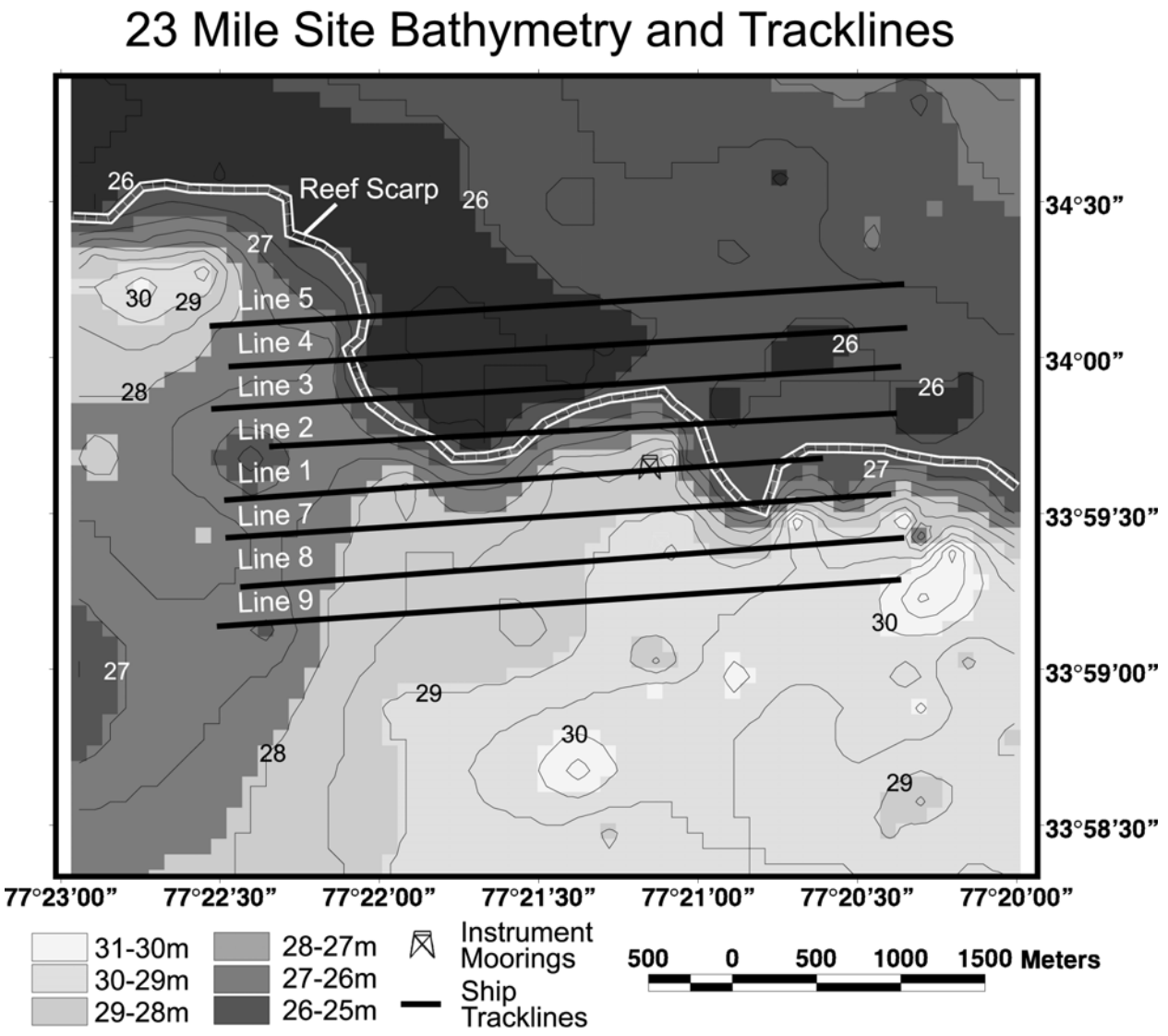
23 Mile Site Bathymetry and Tracklines
Reef Scarp
Line 5
Line 4
Line 3
Line 2
Line 1
Line 7
Line 8
Line 9
26
27
30
29
28
34°30”
34°00”
33°59’30”
33°59’00”
33°58’30”
77°23’00”
77°22’30”
77°22’00”
77°21’30”
77°21’00”
77°20’30”
77°20’00”
31-30m
30-29m
29-28m
28-27m
27-26m
26-25m
Instrument Moorings
Ship Tracklines
500 0 500 1000 1500 Meters

Table 1: Sidescan sonar acquisition parameters for 23 Mile site surveys. * The range of 300m in the 06/2000 survey was twice that of the previous surveys. This was corrected for in post-processing; however, it reduced the across-track resolution by 50%.

SETTINGS	12/1999	12/2000	06/2001	04/2002
Transmit Frequencies (kHz)	100/500(384)	100/500(384)	100/500(384)	100/500(384)
Horizontal Beamwidth (degrees)	100kHz at 1.2^{o} 500kHz at 0.5^{0}	100kHz at 1.2^{o} 500kHz at 0.5^{0}	100kHz at 1.2^{o} 500kHz at 0.5^{0}	100kHz at 1.2^{o} 500kHz at 0.5^{0}
Vertical Beamwidth (degrees)	50^{o} tilted down 20^{0}	50^{o} tilted down 20^{0}	50^{o} tilted down 20^{0}	50^{o} tilted down 20^{0}
Sampling Rate (kHz per channel)	24	24	24	24
Range (m)	150	150	300*	150

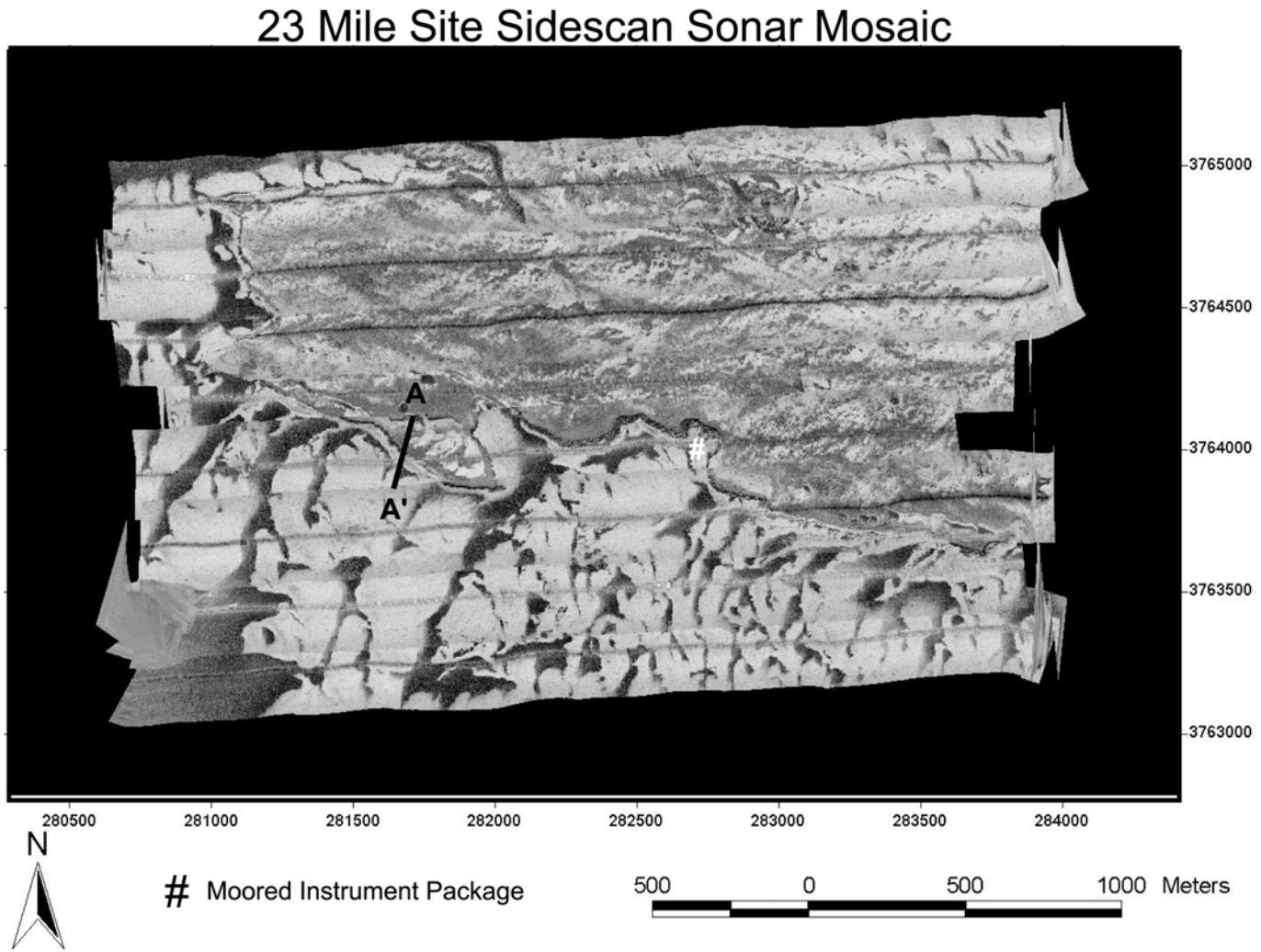

Figure 4: Sidescan sonar mosaic of 23 mile site collected in 12/1999. Areas of high backscatter are shown as dark gray/black, areas of low backscatter are light gray/white. Sonar frequency is 100 kHz. Given 300m swath widths, 100 percent coverage of 2.5 nm by 3.5nm area was achieved. Location of geologic cross-section shown in Figure 2 indicated by thick black line labeled A-A'.

The 12/1999 survey was chosen as the baseline survey to which all subsequent surveys were registered (Fig. 4). Between the four surveys, the lines that contained sections of the reef edge, assumed to be a fixed reference line, (lines 1, 2, 3, 4, 5, and 7) were geographically registered. Lines that did not contain any portion of the reef were mated to the previously corrected lines through overlapping sedimentary features within an individual survey.

Dr. Stan Riggs collected several video segments in 1992, including both diver-assisted videos and submersible-based videos (located at the University of North Carolina-Wilmington's Center for Marine Science in the National Undersea Research Center archives). This footage, in addition to digital video footage collected 11/2002 that confirmed the structures found in the Riggs video, and direct diver observations and sediment sampling were used to groundtruth the sidescan sonar imagery.

Sediment Samples

To assist in the sediment sampling, four transect lines were anchored on the ocean floor stretching north, south, east, and west from the moored instrumented frame. These transects included coarse-grained sand bodies, fine-grained sand bodies, rubble ramp, and the reef edge (Fig. 5). The north and east lines stretched 35m and 25m respectively, where they terminated at the reef edge. The south line stretched 50m where it also terminated at the reef edge. The west line stretched 50m and terminated in the sand flat. The transect lines were marked at one meter intervals (each with a number corresponding to the distance from the frame) allowing for an accurate system of comparing the backscatter

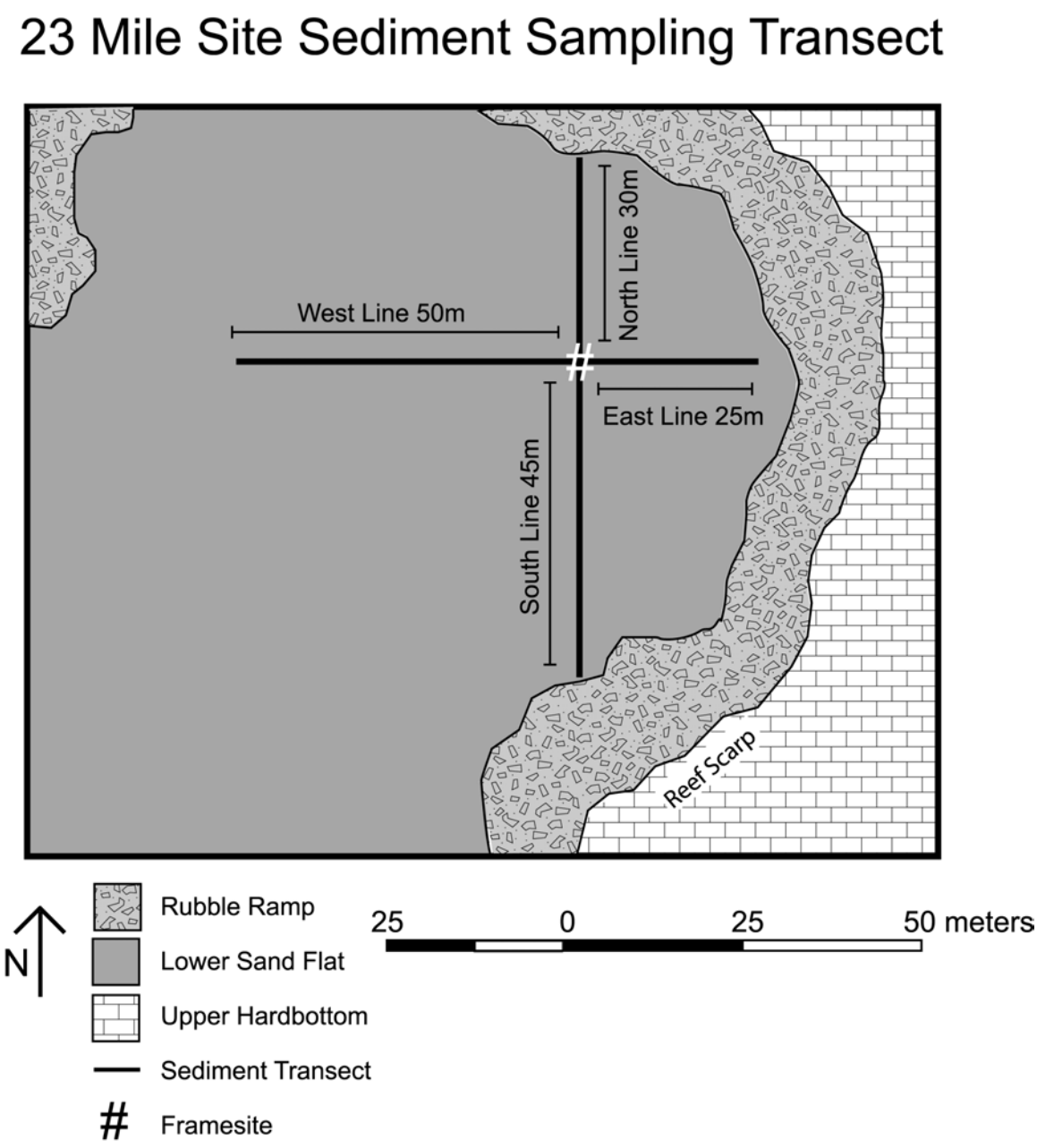

Figure 5: A schematic showing sediment-sampling transect for 23 Mile site and location of CORMP instrument in relation to the reef edge. A transect was anchored onto the seafloor to the north, south, east, and west of the CORMP instrument frame. Grab samples were taken and named according to the line orientation and distance in meters from frame: i.e. sample N20 is located on the north line 20m from the frame, in 5/ 2001, 7/2002 and 9/2002.

intensity to the different sediment types (e.g. fine sand aprons and coarse gravelly sands) and outcrop exposures, and locating sampling stations for repeat measurements (Fig. 5). Surficial grab samples were taken every 5m meters 07/2002 and 09/2002 to examine sediment texture and composition, the extent of sediment reworking and outcrop patterns. An additional series of surficial grab samples were taken before the transect was deployed (05/2001). These samples were taken along the north, south, east and west directions from the frame. The samples were annotated according to their distance and direction from the frame.

Grain-size was determined using dry-sieving techniques (Folk, 1984). Samples were sieved through a set of 1ϕ intervals. The samples were shaken for 10 minutes and then each sieve's contents were weighed. This allowed for the calculation of the mean grain-size for each sample. Mineralogy, presence or absence of shell fragments, and relative sorting of sediment samples were also noted.

RESULTS

Qualitative Analysis of Sidescan Sonar Imagery

Four distinct bottom types were identified qualitatively on the basis of distinctive acoustic characteristics in the sidescan sonar mosaic of 23-mile site (Fig. 6). The four resulting bottom types include: the upper hardbottom, rubble ramp, fine sands, and coarse gravelly sands. These bottom types are closely linked to the seabed habitats initially described by Renaud et al., 1996.

Map of Seabed Types at 23-Mile Site

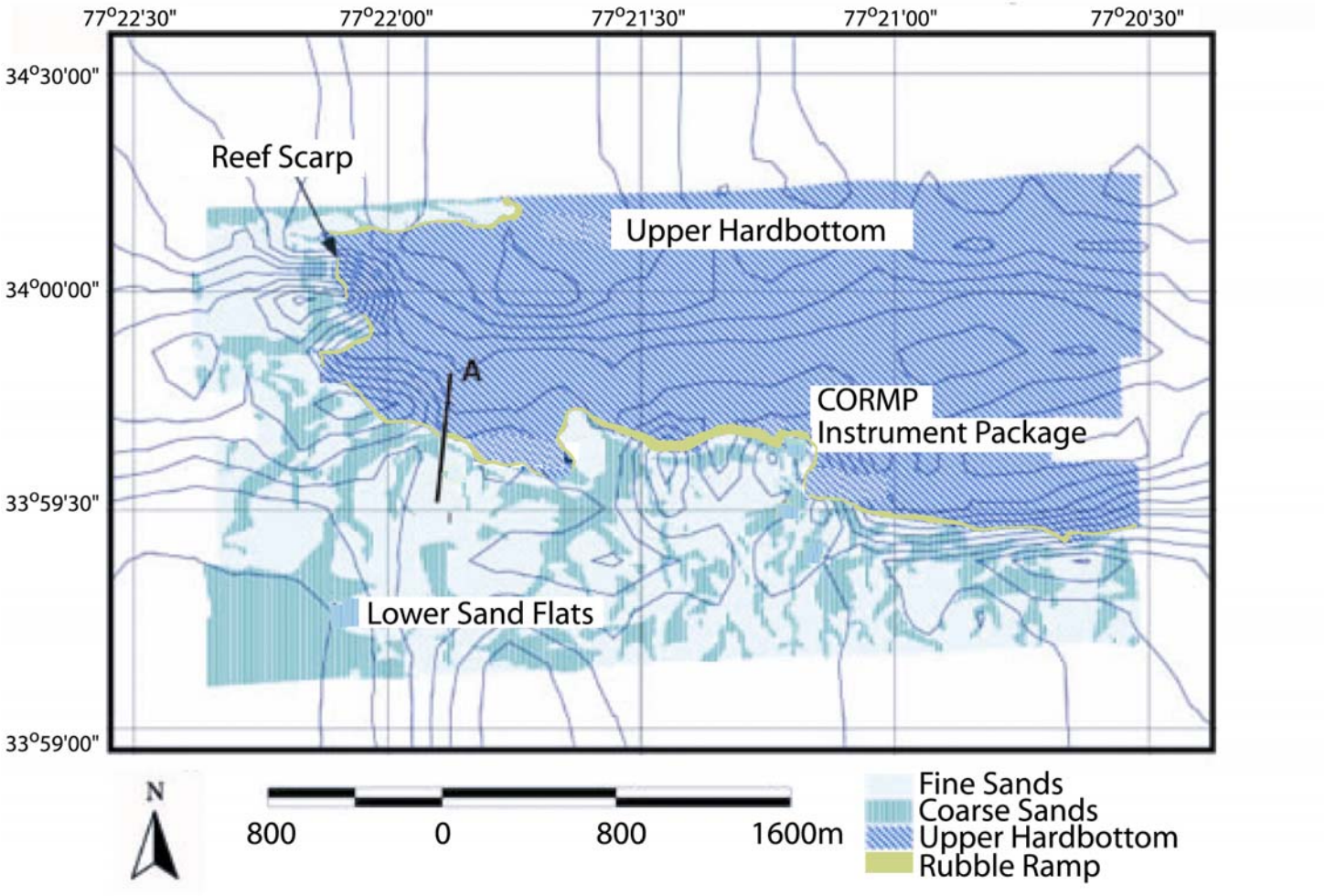

The upper hardbottom, covering approximately 51.5% of the study area, appears as a mottled area of high and low backscatter in the sidescan imagery (Fig.4; 7 a, b). A heterogeneous mix of hardbottom, and thin, fine sand veneers characterizes this area. Diver observations indicate the presence of various macroalgae and other sessile organisms where there is exposed hardbottom. Scattered corals, sponges, and other invertebrates also project through the sand (Renaud, 1997; diver observations). The 5-20m of the upper hardbottom adjacent to the reef scarp is often devoid of sand, providing attachment points for the dense meadows of macroalgae.

In the sidescan imagery, the rubble ramp is a mixture of very distinct high and low backscatter signatures accounting for approximately 4.8% of the total area of the study site (Fig.4; 8a,b). The high backscatter areas are the rubble blocks and the bordering low backscatter areas are their acoustic shadows. The low backscatter areas between rubble blocks may also be fine sands in some instances as video and diver observations have revealed. The rubble ramp ranges in width from 5m to more than 30m from the scarp to edge of the furthest rubble blocks. The scarp itself appears in the sidescan imagery as a distinct boundary between the mottled upper hardbottom and the blocky high/low backscatter contrasts of the rubble ramp. Diver observation and video, indicate dense populations of marine life found immediately adjacent to the reef scarp and rubble ramp complex.

In the sidescan imagery, the lower sand flat is characterized by alternating, north-south trending high and low backscatter areas (Fig. 4). The high backscatter areas mark the coarse-gravelly sands (Fig. 9a,b), and the fine sands are depicted by low backscatter returns (Fig. 10a,b). The lower sand flat accounts for approximately 43.7% of the study

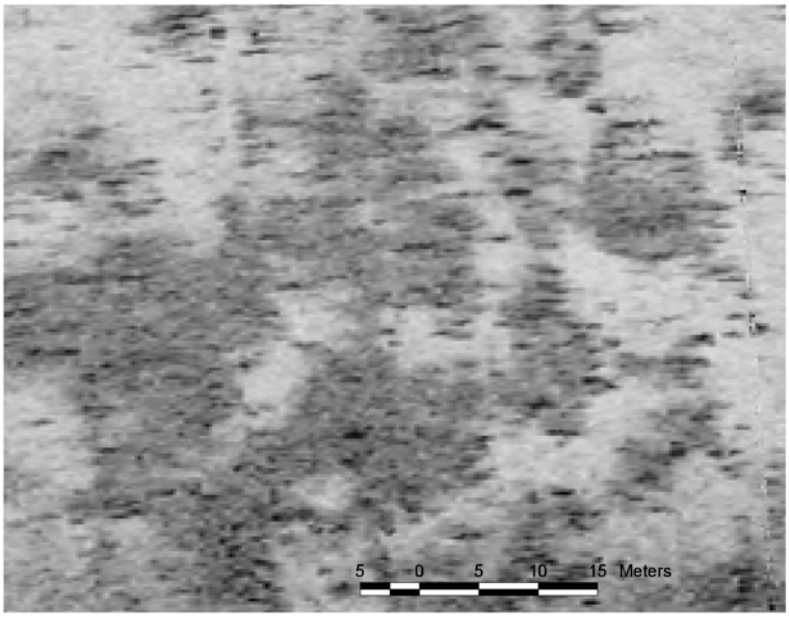

Figure 7 a: Upper hardbottom video clip and sidescan sonar image showing the relationship of the seafloor to the sidescan sonar backscatter. The video clip shows abundant brown macroalgae Species composition of brown macroalgae at 23-Mile varies year to year but may include *Sargassum filipendula*, *Zonaria tournefortii*, *Lobophora variegata*, *Sporochnus pedunculatus*, *Codium isthmocladum*, and *Dictyopteris hoytii*.

b: The mottled appearance in the sidescan, however, is a result of the fine sand sheets and the exposed hardbottom. The small dark returns appear to be scattered coral heads (tic corals), rock outcrops, and/or large sponges (i.e. vase sponges).

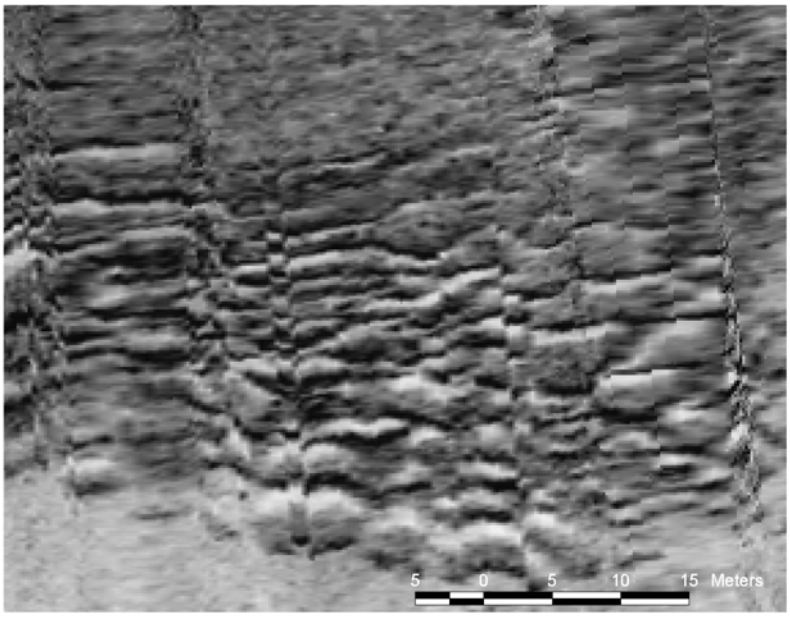

Figure 8 a: Rubble Ramp video clip and sidescan sonar image showing the relationship of the seafloor to the sidescan sonar backscatter. The video clips shows the large blocks (up to 5m x 10m) covered with dense brown macroalage (and other biota?)

b: The checkered appearance in the sidescan is a result of the large rubble blocks lying immediately adjacent to the reef scarp. The rubble ramp ranges in width from 5m to more than 30m from the scarp to edge of the furthest rubble blocks.

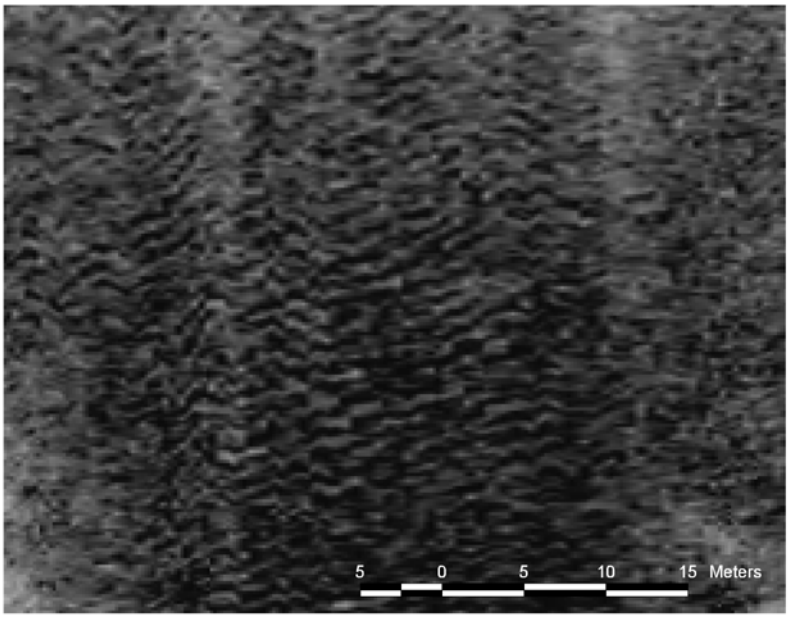

Figure 9 a: Coarse sands video clip and sidescan sonar image showing the relationship of the seafloor to the sidescan sonar backscatter.

b: The striated appearance of the coarse sand body in the sidescan is a result of the megaripples with wavelengths of ~1m (seen in the video clip), which are present only in the coarse sands.

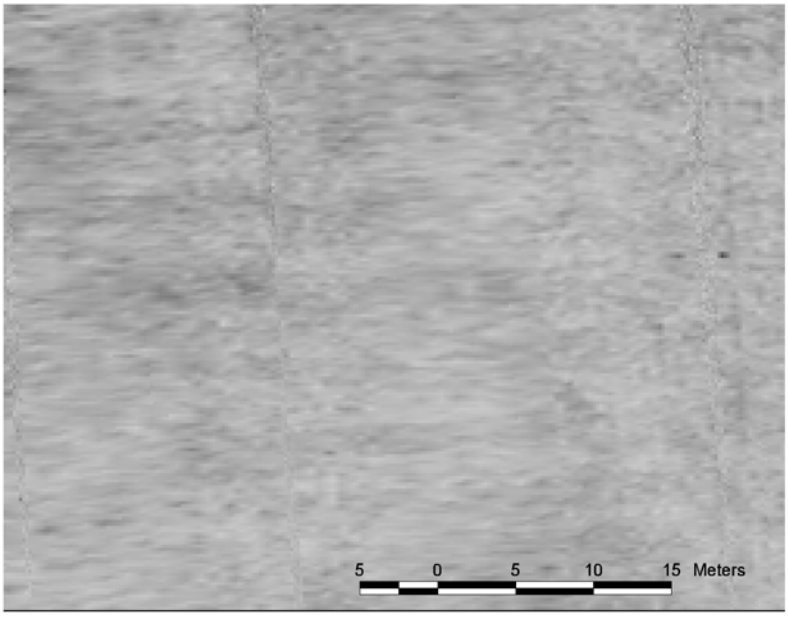

Figure 10 a: Fine sands video clip and sidescan sonar image showing the relationship of the seafloor to the sidescan sonar backscatter. Video clip shows small ripples (with wavelengths from 3-30cm and wave heights of 0.5-2cm) in the fine sands, which are not discernable in the sidescan imagery.

b: The relatively homogenous texture in the sidescan is due to the lack of other reflectors or resolvable seabed texture.

area. The north-south trending, alternating bands of high and low backscatter vary from < 5m in width to greater than 400m. The majority of the sand flat is marked by low backscatter (fine sand) bands, with narrower, less contiguous bands depicted by high backscatter (coarse sand) returns. These delineations between the fine and coarse-grained sands are much more difficult to discern during diver observations. The most notable difference to the unaided eye is the megaripples (wavelength=~1m) found within the coarse sand bodies. In box cores taken in the lower sand flat, the fine sands are present above cross-bedded coarse sand fractions suggesting that the fine sands are moving across the coarse sand bodies.

Sediment Analysis

In the lower sand flats, samples were deemed to be coarse or fine based on their mean grain size. Sediment samples with greater than 0.38mm mean grain size were deemed coarse, while those with mean grain sizes of less than 0.38mm were deemed fine. The coarse and fine samples were very distinct with no samples showing a transitional mean grain size. The fine sands were moderately well-sorted and consisted primarily of silicates with fine pieces of carbonate material (Fig. 11). The coarse samples were poorly-sorted. The coarse samples had a silicate sand presence, and these samples also had greater carbonate content than the fine samples. This coarse fraction consisted of shell fragments, coral fragments, and pieces of the reworked limestone scarp (Fig. 12). The grain size of the coarse and fine grain sands were averaged using one ϕ intervals and two histograms were constructed to show the typical coarse sample characteristics and

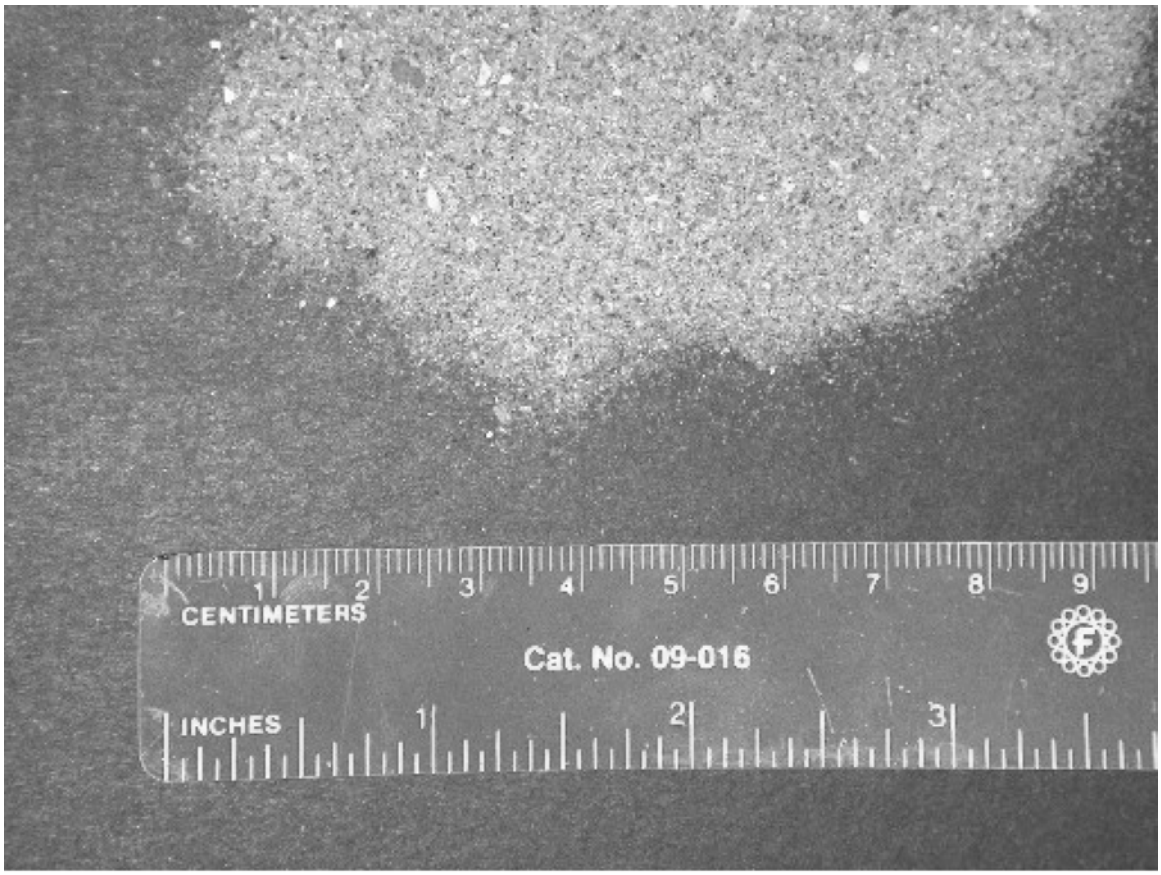

Figure 11: A digital photo of a typical grab sample from a fine-grained sand body showing few shell fragments and fine, well-sorted grains. The average grain size for the fine sand bodies was 0.22mm.

Figure 12: A digital photo of a typical grab sample from a coarse-grained sand body showing numerous large shell fragments, poor sorting. The average grain size computed for the coarse samples was 0.63mm. This is an underestimate for the coarse sands as the coarsest sieve was a 2mm sieve, and there were many pieces far larger than that; this method, however, was sufficient to differentiate between the coarse and fine sand bodies.

fine sample characteristics (Figs. 13 & 14). The mean grain size of the coarse sands is 0.63mm. The mean grain size of the fine sands was 0.22mm.

Sidescan Textural Analysis

On the basis of the qualitative analysis of the sidescan sonar imagery, four distinct groundtruthed seabed types were identified for this study. From these areas, one 96 X 96 pixel (24 m by 24 m) areas of each seabed type was chosen for textural analysis (Fig. 15). These areas were analyzed using the GLCM algorithm developed by Tso and Mather (2001) (Appendix B). The GLCM analysis produces five output files: Angular Second Moment, Entropy, Inverse Difference Moment (homogeneity), Contrast, and Correlation. The indices of entropy and homogeneity (idm) used in this study followed those used by Blondel and Shokr in previous studies (Blondel et al., 1998 Shokr et al., 2001). Raw values of pixel gray-level were chosen as a third parameter for classification.

The output from the GLCM analysis was graphed in three dimensions that included axes of homogeneity, entropy, and gray level value. The graph, shown in figure 16, shows three of the four bottom types appearing distinctly as separate clusters (Fig. 16). The GLCM analysis provided a testable three-dimensional range for each of the seabed types (Table 2).

A wide range of homogeneity values characterized the upper hardbottom. These are due to its mottled backscatter signature (Table 2). There were vast areas of fine sands, which resulted in high homogeneity values, while the hardbottom returns resulted in relatively low homogeneity values. The upper hardbottom had highest entropy values due to the high variability in the sidescan signature and the distinct lack of

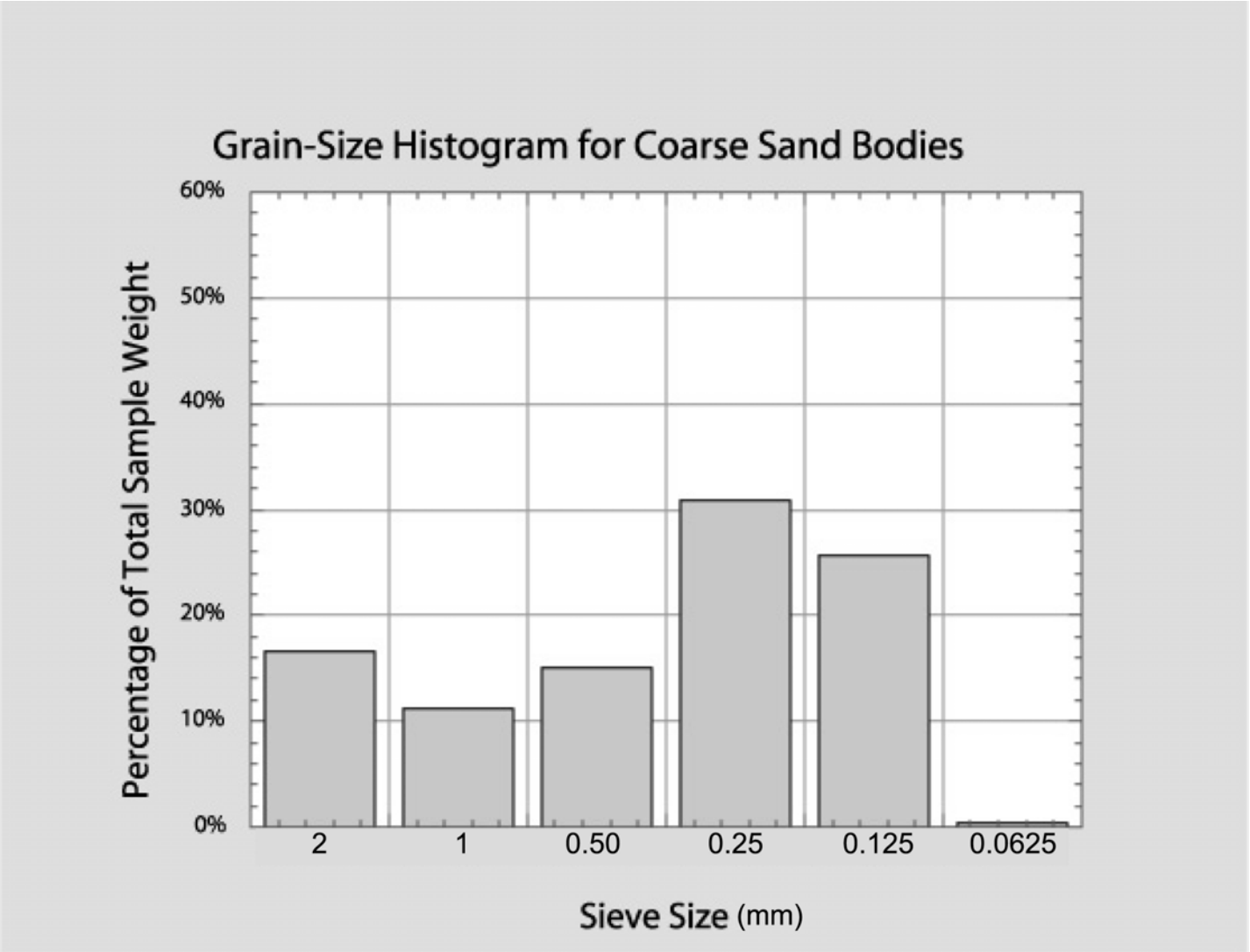

Figure 13: Histogram of coarse sand bodies. This was constructed by taking the mean of the samples that were deemed to be coarse.

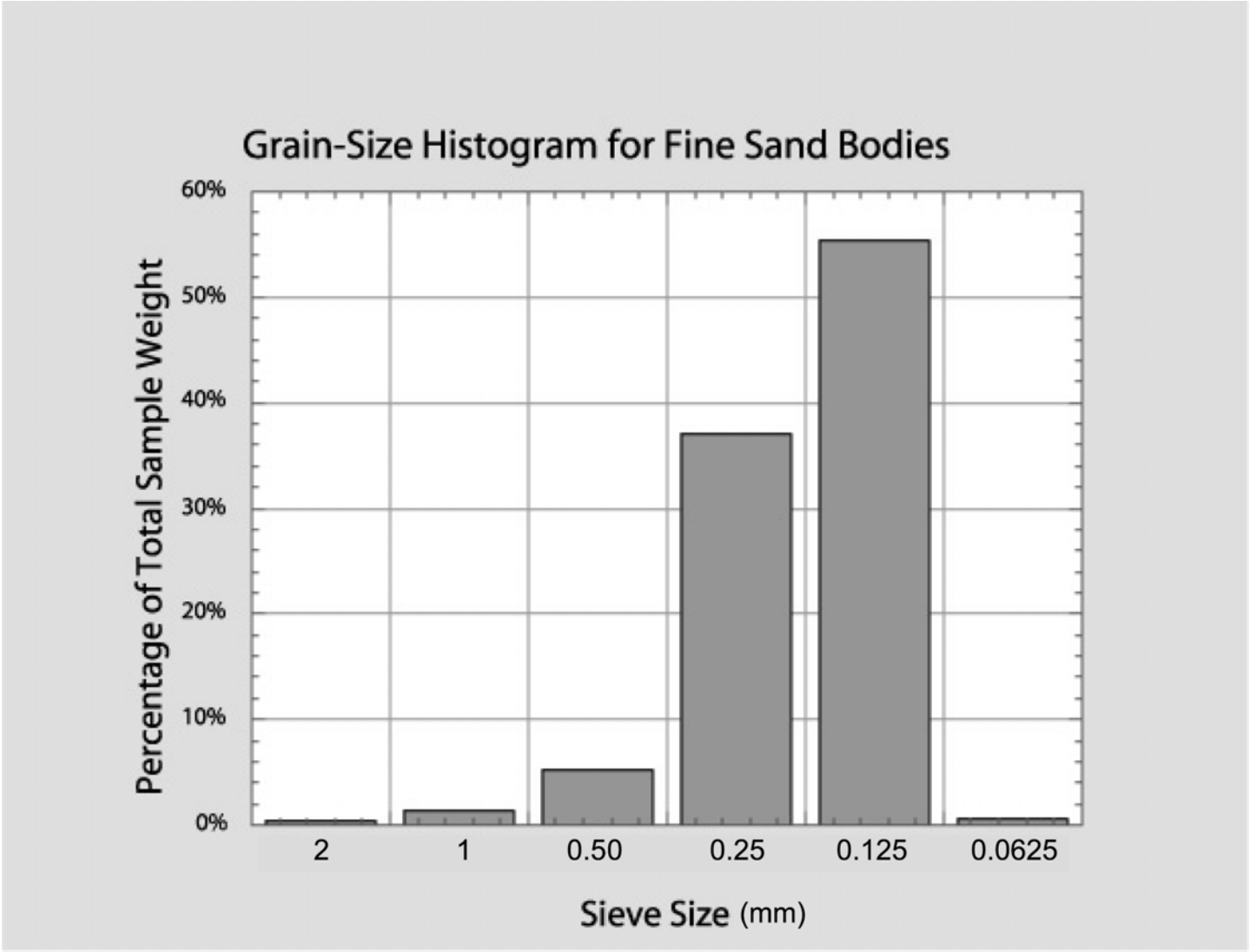

Figure 14: Histogram of fine sand bodies. This was constructed by taking the mean of the samples that were deemed to be fine.

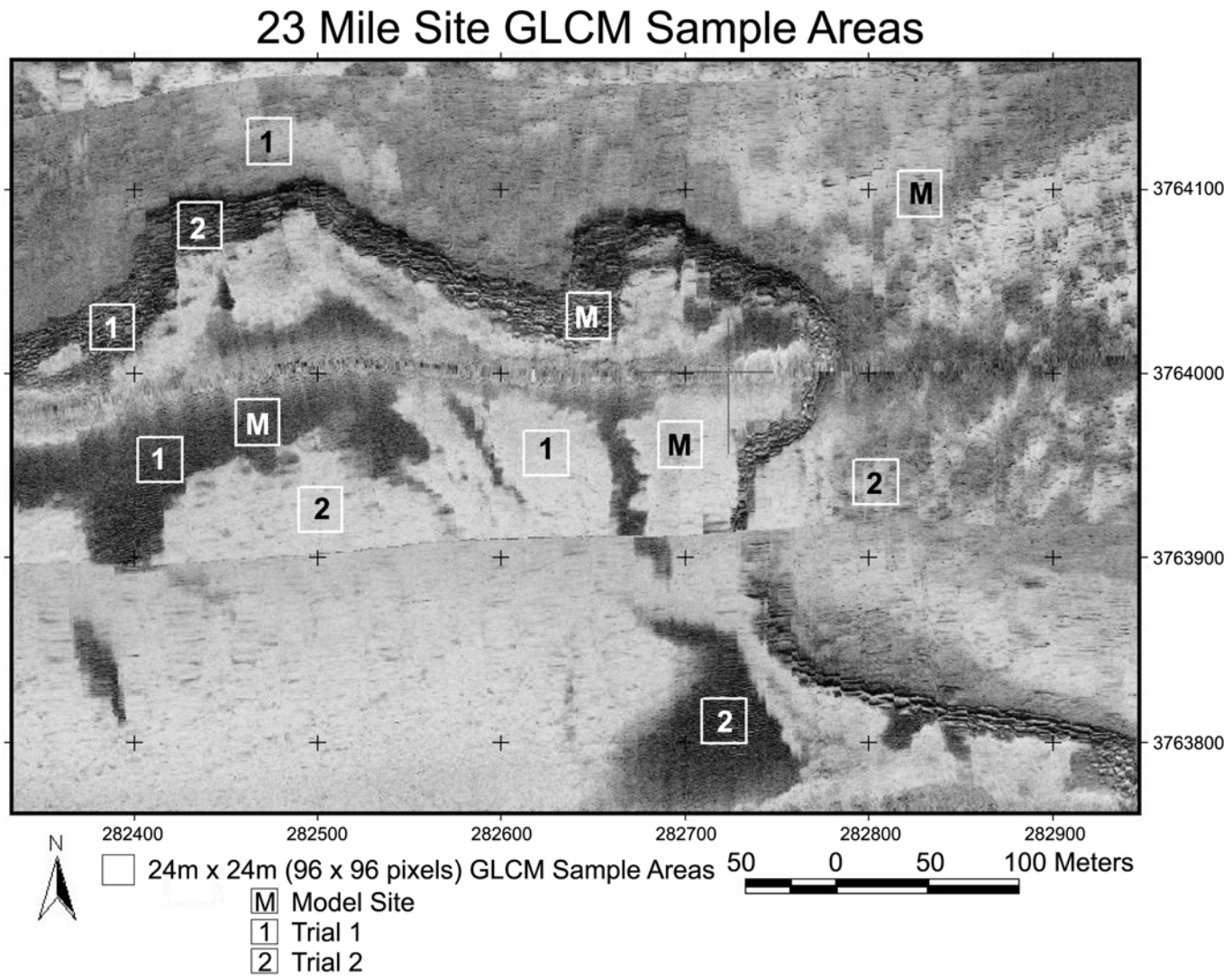

Figure 15: 23 Mile frame area showing samples locations used in the GLCM analysis. Each sample area is 96 x 96 pixels (24m x 24 m). Black boxes represent the four model sites. The eight white boxes represent the two trial sites for each identified bottom-type. 12/99 mosaic shown.

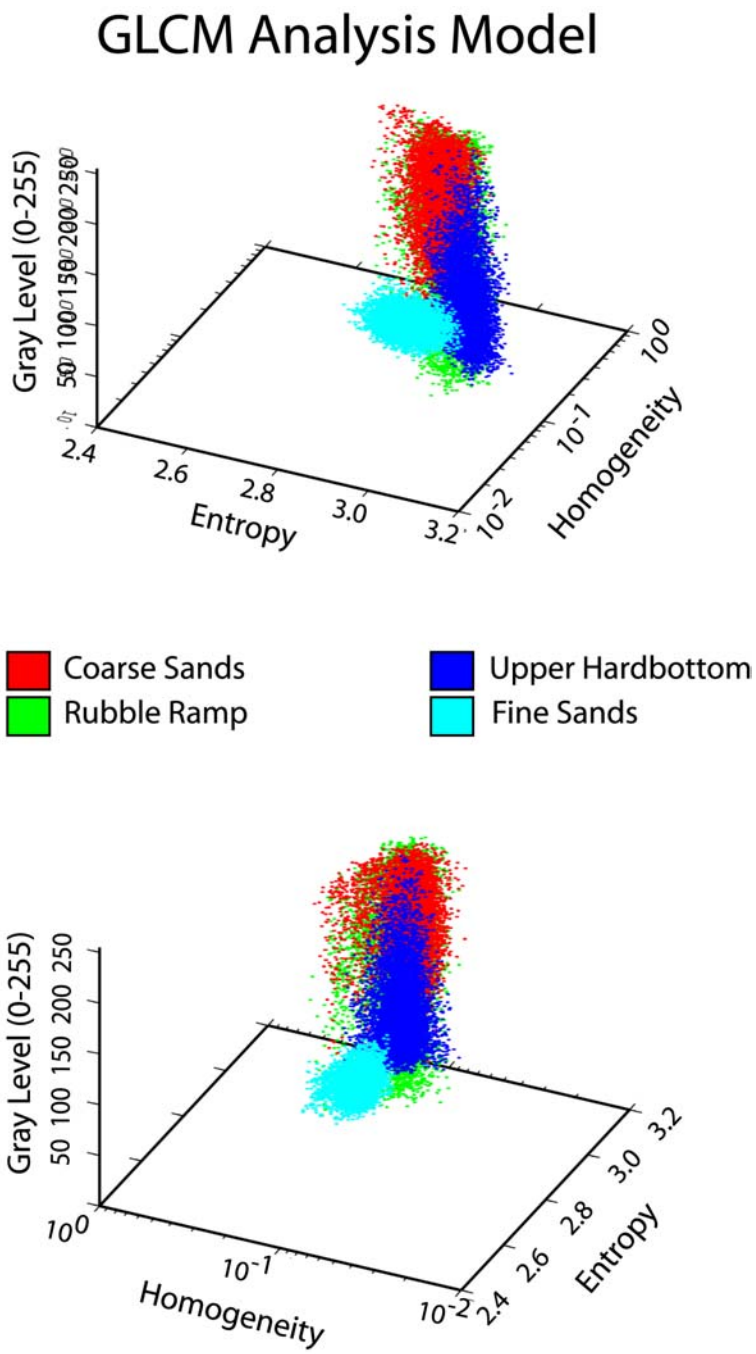

Figure 16: GLCM analysis graphed in three dimensions showing the grouping of the four seabed types: fine sands, coarse sands, rubble ramp, and upper hardbottom. The upper hardbottom had the highest entropy values and a large range in gray scale values. The fine sands were found to have the lowest entropy values and highest homogeneity grouping with little variation in gray level. The coarse sands had relatively low entropy values and the lowest homogeneity values. The rubble ramp had high entropy values, but low homogeneity and large variability in gray level values. The values for the rubble ramp occupied the ranges of the upper hardbottom and coarse sands as well. This made it very difficult to differentiate the rubble ramp from the coarse sands and rubble ramp.

Table 2: GLCM analysis seabed classification values showing three-dimensional differentiation between the four seabed types. There are vast areas of fine sands, which result in high homogeneity values, while the hardbottom returns result in relatively low homogeneity values. The upper hardbottom had highest entropy values due to the high variability in the sidescan signature and the distinct lack of textural organization. The rubble ramp, due to its heavy contrast and relatively organized pattern, resulted in high entropy values. The great disparity in gray level values is a result of the hard and soft returns as well as the acoustic shadows resulting from the rubble blocks. This wide range of values resulted in low homogeneity values. The fine sands were found to have the lowest entropy values, as there is little textural roughness. The sonograph shows very little variability in the backscatter intensities within the fine sand bodies, resulting in the highest homogeneity values of the group. The coarse sands had a relatively low entropy value, and had the lowest homogeneity value as well.

Bottom Type	Entropy	Homogeneity	Gray-Level
Upper Hardbottom	2.86-3.14	0.062-0.231	10-251
Rubble Ramp	2.78-3.12	0.054-0.191	8-253
Coarse Sands	2.78-3.11	0.045-0.196	58-252
Fine Sands	2.73-3.02	0.08-0.227	22-102

textural organization. The rubble ramp due to its heavy contrast and relatively organized pattern resulted in high entropy values. The great disparity in gray level values is a result of the hard and soft returns as well as the acoustic shadows resulting from the rubble blocks. This wide range of values resulted in low homogeneity values. The patterns created by the rubble blocks, though distinct, were found to have a range of values that intersected both the upper hardbottom values and the coarse sand values. The rubble ramp had entropy values nearly identical to the coarse sands. The homogeneity values of these seabed types were also very similar. The rubble ramp cluster; therefore, was not discernible from the other three bottom types. For this reason the rubble ramp will not be used in the preliminary classification scheme.

The fine sands were found to have the lowest entropy values, as there is little textural roughness. The sonograph exhibited very little variability in the backscatter intensities within the fine sand bodies, resulting in the highest homogeneity values of the group.

The coarse sands had a relatively low entropy value. They had the lowest homogeneity value as well. Though they were relatively homogeneous over a large spatial scale, the short run length of the GLCM vectors only took into account pixels over a 3.75m distance (this is value d, as defined in Appendix B). On this scale, the coarse sands were the least homogenous due to the megaripples. The backscatter signature of these ~1m features created a very heterogeneous profile.

To test the models GLCM relationships, two additional 96 x 96 pixel (24 x 24m) samples of each bottom type were chosen from different areas within the mosaic (Figs 15 & 16). These areas were independently analyzed and output from these analyses was

graphed against the clusters generated by the model (Figs. 17, 18, 19, & 20). In all cases GLCM analysis was capable of differentiating each of the four bottom types regardless of location within the mosaic. Each of the four analyses showed nearly identical results for the two trial samples that closely matched the model.

Change Detection Analysis

The change detection analysis focused primarily on the lower sand flats due to the highly visible contacts of the various sand bodies. Five areas with distinct high/low backscatter signatures were chosen to measure sediment displacement between successive mosaics (Fig 21): These subareas are labeled as LSF-#, with LSF representing lower sand flat. The subareas were labeled with numbers increasing from west to east (Fig. 21). Three areas were chosen in the expansive sand flat to the south (LSF-2, 3 & 5), one area (LSF-4) adjacent to the framesite was chosen, and one area (LSF-1) to the west of the reef ledge was chosen. These areas were chosen to determine if proximity to the reef ledge caused differentiating trends in the fine/coarse sand boundary migration.

Because of the error associated with the DGPS measurements and uncertainty in the fish location an error buffer was created around each of the digitized fine/course sand contacts (Fig. 22). Displacements between mosaics beyond the error buffer were considered to be significant. The areas of total displacement were calculated using the *Intersect Themes* and *Calculate Area* functions within the ArcView XTools extension (Fig. 23). The areas were summed, the difference was then halved and the spatial displacement was attained. Displacement direction and magnitude were also noted.

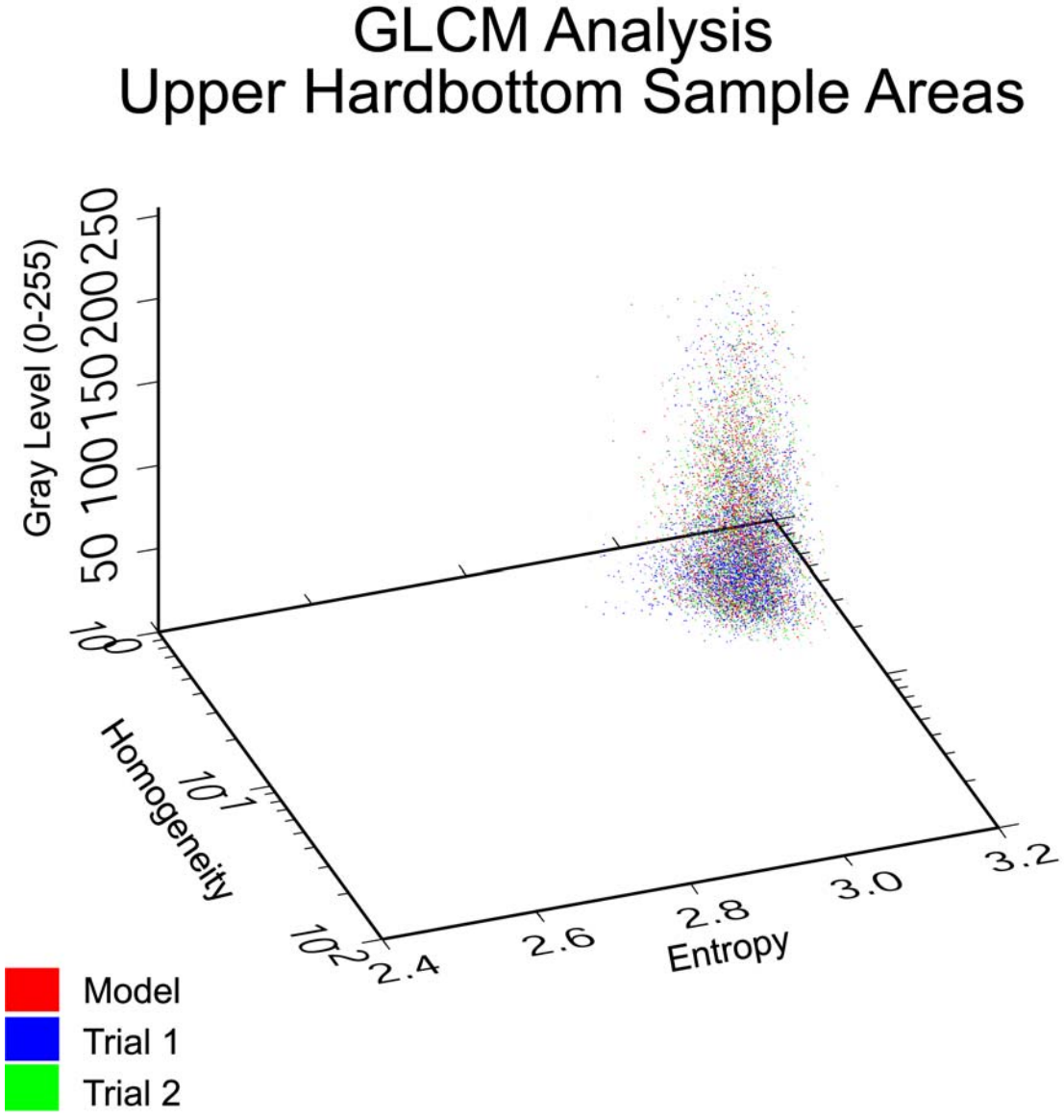

Figure 17: Upper hardbottom GLCM analysis showing a tight clustering of model and trial samples.

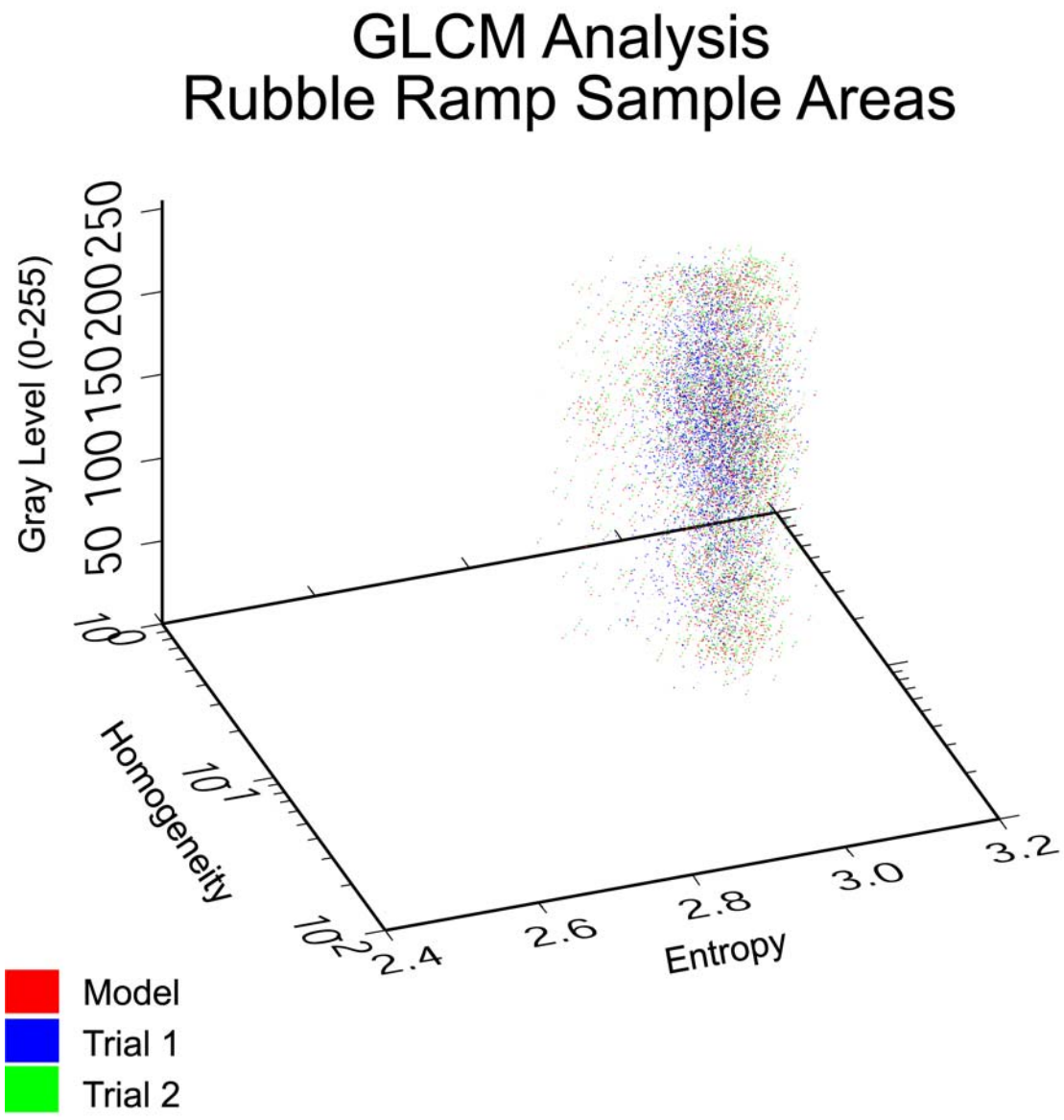

Figure 18: Rubble ramp GLCM analysis showing a tight clustering of model and trial samples.

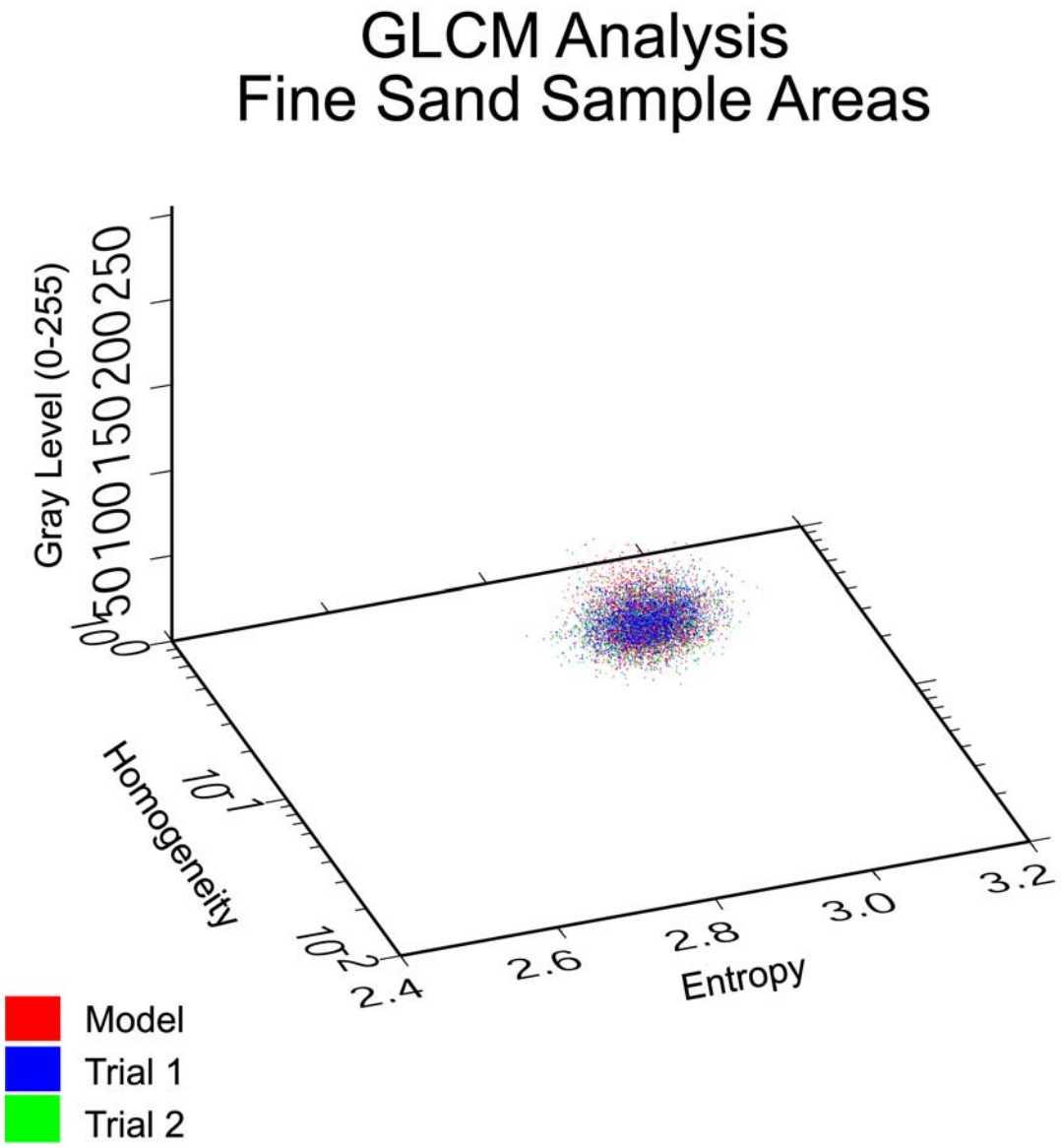

Figure 19: Fine sand body GLCM analysis showing a tight clustering of model and trial samples.

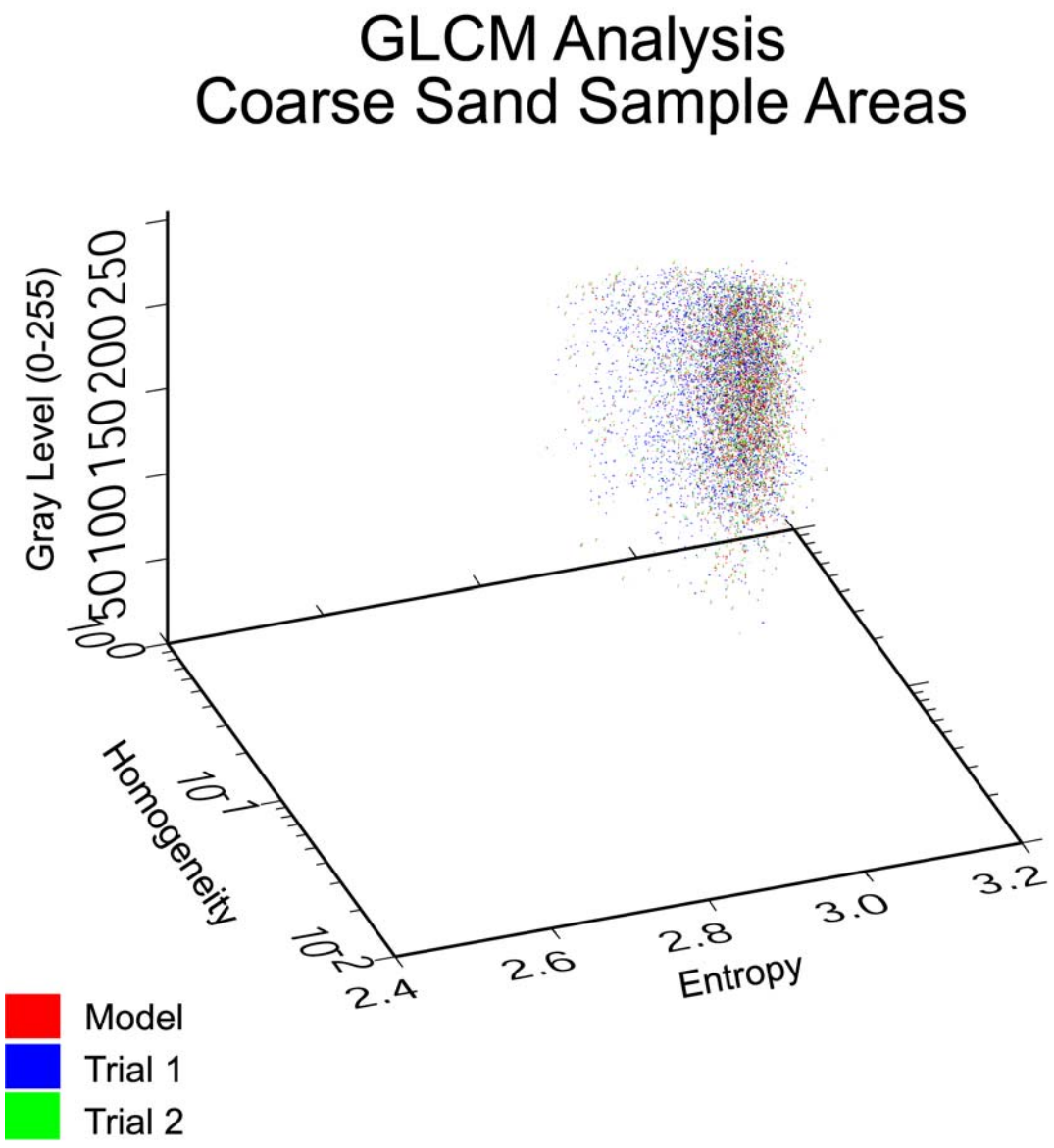

Figure 20: Coarse sand body GLCM analysis showing a tight clustering of model and trial samples.

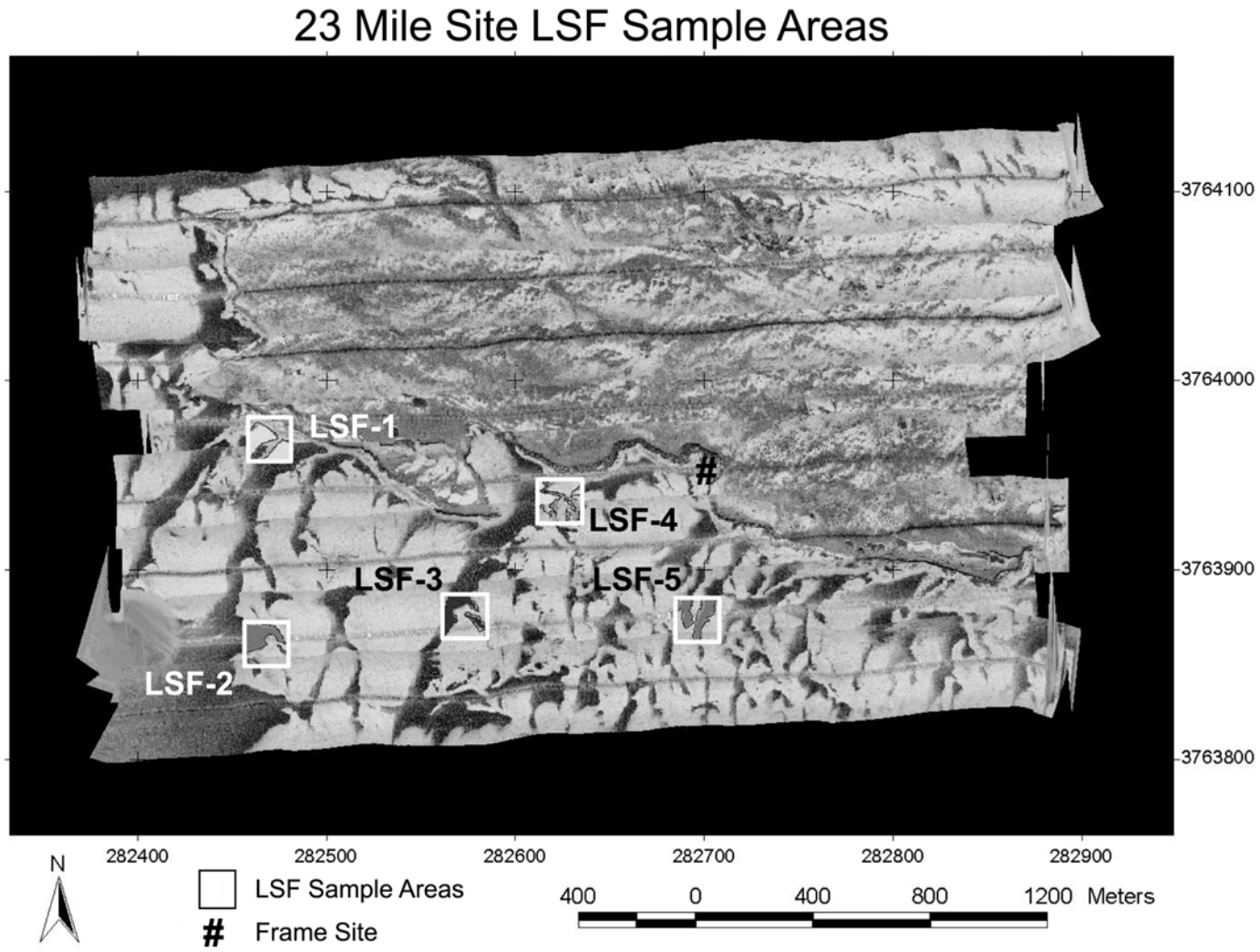

Figure 21: 23 Mile sidescan mosaic (12/1999) showing Lower Sand Flat (LSF) study areas. These five areas were chosen for the change detection analysis. Within each of these areas, the high/low backscatter contacts were digitized so that these positions could be compared over time.

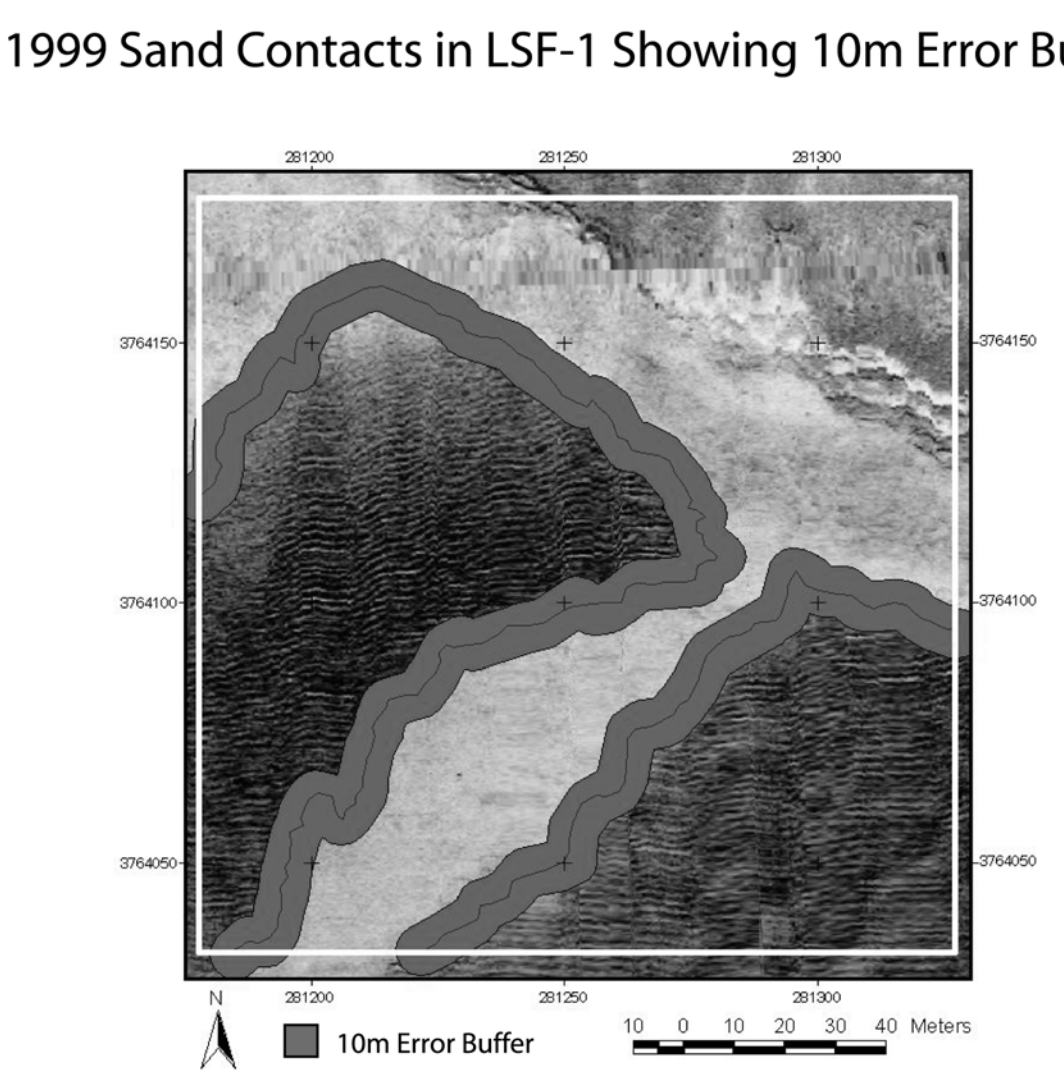

Figure 22: Error buffer along course-fine grain contacts displaying +/- 10m error tolerance used in the area displacement calculations.

1999-2000 Sand Contact Displacement at LSF-1

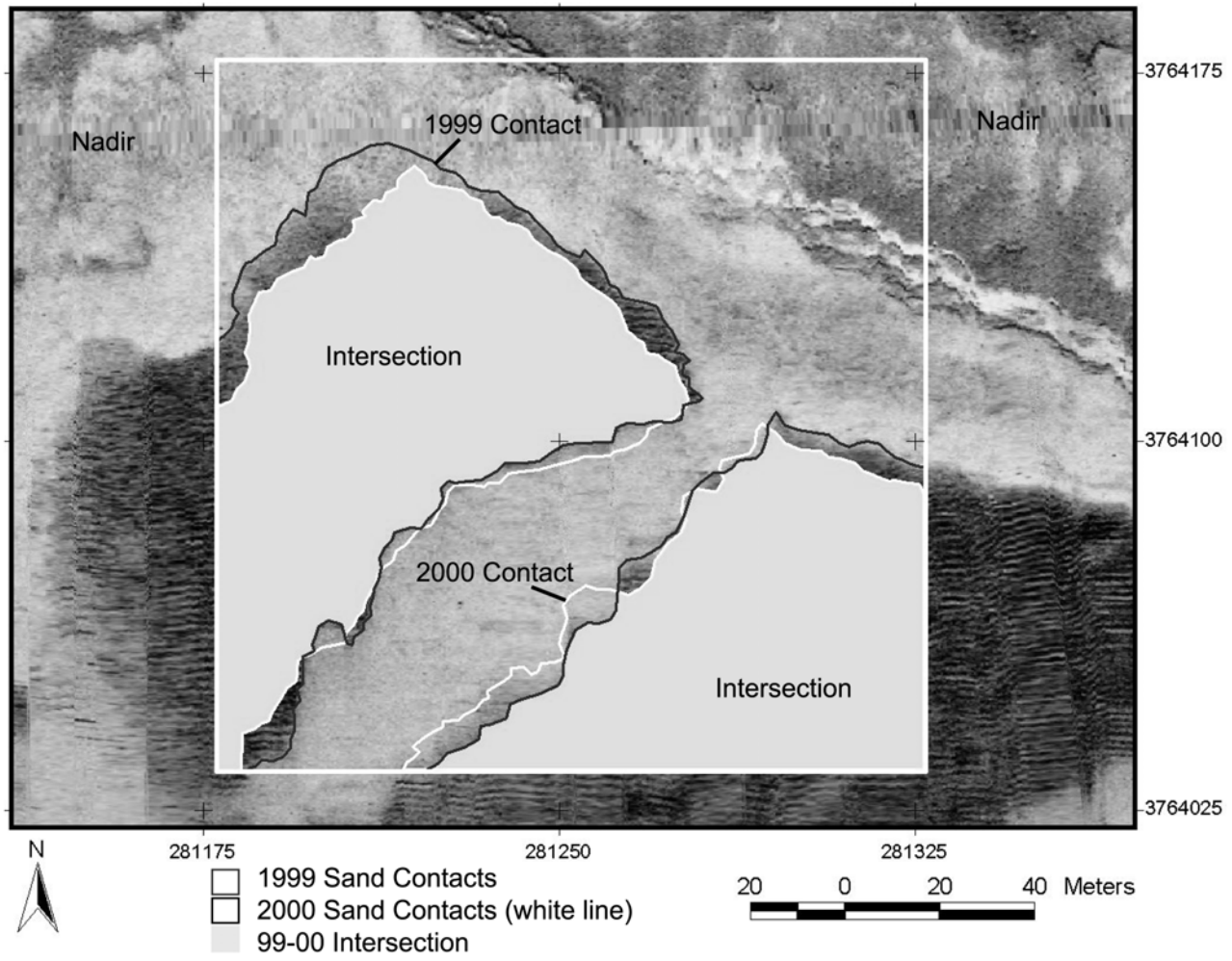

The displacements for the 12/1999-12/2000, 12/2000-06/2001, and 12/1999-06/2001 survey periods were calculated. The 04/2002 survey was not used in the GIS analysis because of sea conditions during the survey. The pitching of the ship was translated into increased pitch for the towfish. This resulted in significant noise in the backscatter signature. Therefore, it was not possible to digitize the boundaries between the high and low backscatter features within the 10m error tolerance.

Lower Sand Flat Subarea One (LSF-1)

The LSF-1 subarea is located immediately adjacent to the reef ledge approximately 55m from the westernmost boundary of the study area. At this site, the reef ledge is facing southwest. This subarea is completely contained within line 4 of the sidescan surveys. From 1999-2000 contact shifts showed a consistent shift of all boundaries to the southeast, totaling 1741 m^2 (Table 3). The displacement of the westernmost boundary of this subarea was significant as it exceeded the buffer, with a horizontal displacement of up to 14m. Other boundaries showed movement of 0-8m laterally. From 2000-2001, the boundary shifts were mixed and showed a slight shift to the northeast along several portions of the boundaries. The overall displacement was 1155m^2. This shift did not exceed the error tolerance buffers. The net shift from 1999-2001 was 1487m^2. The displacement was in an eastern to south-southeastern direction and exceeded error tolerance buffers in portions of the boundaries similar to those seen in the 1999-2000 study.

Table 3. LSF-1 sand displacement and direction

LSF-1 Sample Year	Coarse Sand Area (m^2)	Displacement from '99 (m^2) & Direction	Displacement from '00 (m^2) & Direction	Displacement from '01 (m^2) & Direction
1999	11421	n/a	1741 SE	1487 E
2000	10677	1741 SE	n/a	1155 NE
2001	11009	1487 E	1155 NE	n/a

Lower Sand Flat Subarea Two LSF-2

The LSF-2 subarea is located 700m south of LSF-1. LSF-2 is 570m from the nearest portion of the reef ledge. This subarea is located entirely within line 7 of the sidescan surveys. The 1999-2000 contact shifts showed a consistent shift across all boundaries to the south (Table 4). The overall displacement was 2430m^2, and showed significant displacement at several locations along the boundaries. The 2000-2001 analysis revealed a consistent 1913m^2 shift to the north; however, this shift did not exceed the error tolerance buffers. The net overall shift from 1999-2001 was 1287m^2 shift to the south. This shift was consistent throughout the sand body, but the error tolerance buffers are not exceeded, as there was very little displacement.

Lower Sand Flat Subarea Three (LSF-3)

The LSF-3 subarea is located 525m east of LSF-2 and 250m south of the nearest portion of the reef ledge. LSF-3 is located within lines 6 and 7 of the sidescan surveys. The 1999- 2000 contacts showed a significant displacement of 2458m^2 (Table 5). The displacement across most portions of the boundaries was consistent in the south-southeast direction. The boundaries in the westernmost corner of the subarea showed a significant shift to the west and northwest. The morphology of these contacts changed significantly as well. The 2000-2001 analysis revealed a displacement of 1497m^2. The minimal displacement exhibited a consistent shift to the north. This period exhibited minimal morphologic change. The 1999-2001 net displacement was 1833m^2, and showed significant morphological change in the contacts. However, there was no consistent direction of displacement.

Table 4. LSF-2 sand displacement and direction

LSF-2 Sample Year	Coarse Sand Area (m^2)	Displacement from '99 (m^2) & Direction	Displacement from '00 (m^2) & Direction	Displacement from '01 (m^2) & Direction
1999	9309	n/a	2430 S	1287 S
2000	9041	2430 S	n/a	1913 N
2001	8895	1287 S	1913 N	n/a

Table 5. LSF-3 sand displacement and direction

LSF-3 Sample Year	Coarse Sand Area (m^2)	Displacement from '99 (m^2) & Direction	Displacement from '00 (m^2) & Direction	Displacement from '01 (m^2) & Direction
1999	9100	n/a	2458 SE	1833 N
2000	9943	2458 SE	n/a	1497 SE
2001	9383	1833 N	1497 SE	n/a

Lower Sand Flat Subarea Four (LSF-4)

The LSF-4 subarea is located 300m northeast of LSF-3 and 400m west of the framesite. LSF-4 is located immediately adjacent to the reef ledge and is contained entirely within line 5 of the sidescan surveys. The 1999-2000 contacts showed significant displacement of 4450m^2 to the east (Table 6). This shift was greater in the southern portion of the subarea. The 1999-2000 surveys revealed a significant morphological change in the high/low backscatter contacts. The 2000-2001 analysis revealed consistent displacement in the western direction of 2531m^2. There was minor morphological change during this time period. The net displacement from 1999-2001 was 3399m^2 in an eastern direction. This survey again showed significant displacement in the southern portion of the subarea and significant morphological change of the high/low backscatter boundaries.

Lower Sand Flat Subarea Five (LSF-5)

The LSF-5 subarea is located 425m south of the framesite and 260m from the nearest portion of the reef ledge. LSF-4 is 650m east of LSF-3 and is contained entirely within line 7 of the sidescan surveys. The 1999-2000 surveys revealed a 2586m^2 displacement in an east-southeast direction (Table 7). This time period exhibited a significant displacement across many of the contacts. However, there was little morphological change in the high/low backscatter boundaries during this time period. The 2000-2001 analysis revealed a displacement of 1753m^2. This displacement showed little consistency in direction. There was a notable shift in some areas to the northwest, though this shift did not exceed the error tolerance buffers. The net displacement between 1999-2001 was 1949m^2 to the east. The shift exceeded the tolerance buffers in

Table 6. LSF-4 sand displacement and direction

LSF-4 Sample Year	Coarse Sand Area (m^2)	Displacement from '99 (m^2) & Direction	Displacement from '00 (m^2) & Direction	Displacement from '01 (m^2) & Direction
1999	5880	n/a	4450 E	3399 E
2000	7246	4450 E	n/a	2351 W
2001	6633	3399 E	2531 W	n/a

Table 7. LSF-5 sand displacement and direction

LSF-5 Sample Year	Coarse Sand Area (m^2)	Displacement from '99 (m^2) & Direction	Displacement from '00 (m^2) & Direction	Displacement from '01 (m^2) & Direction
1999	9401	n/a	2586 SE	1949 E
2000	8795	2586 SE	n/a	1753 NW
2001	8813	1949 E	1753 NW	n/a

only three localized areas. The remainder of the contacts showed no significant displacement. This time period exhibited moderate morphological change.

DISCUSSION

Relationship of Seabed Properties to Sidescan Backscatter Signal

One goal of this study was to determine the relationship of backscatter signal returns to various seabed properties. These properties include grain size, carbonate content, biota, and subsurface structures.

Grain Size vs. Backscatter Intensity

Several studies (Ryan and Flood, 1996; Goff 1999, 2000; LeBlanc et al., 1995; Davis et al., 1996) have noted the importance of sediment grain size to the sidescan sonar acoustic backscatter. A rougher surface will scatter acoustic energy more effectively. This relationship was evident when comparing mean grain size of the high backscatter areas to the low backscatter areas. The grab samples from the frame transect allowed for a direct sampling of the high and low backscatter bodies (Fig. 24). Each sample's mean grain size was then graphed against the backscatter intensity of the 06/2001 survey. The 04/2002 survey, although closest to date of the majority of the sediment samples, is of insufficient quality to extract the required backscatter intensity data. For this reason the mean grain sizes (from samples collected in 05/2001, 07/2002, and 09/2002) were graphed against backscatter data from the 06/2001 survey. These graphs were used to show that the high backscatter features correspond to the coarse samples and the lower backscatter samples correspond to the fine sand samples on the transect.

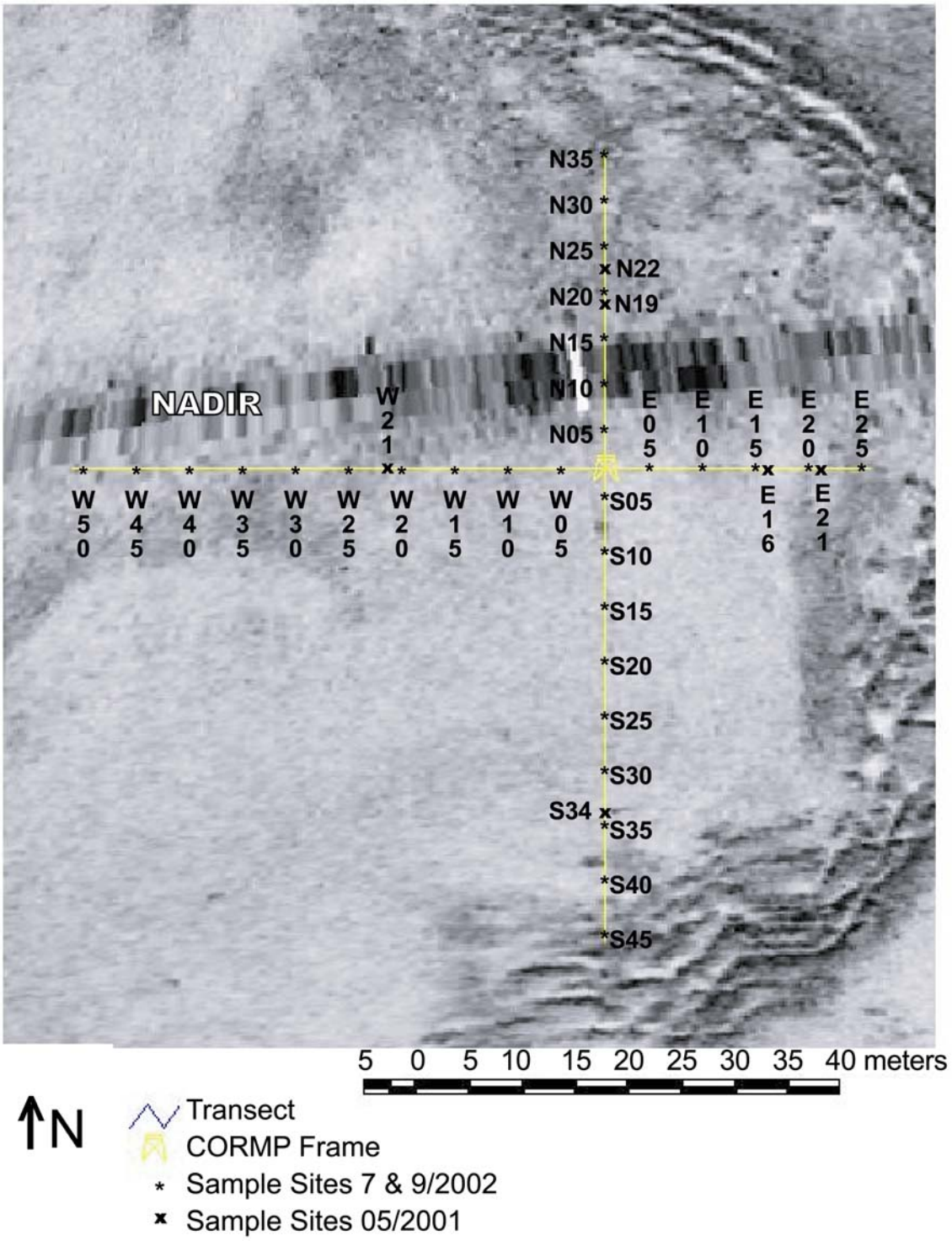

Figure 24: Sediment sampling transect overlaid on sonograph collected 06/2001, showing the nomenclature for the sampling sites. Sampling sites are labeled according to direction and distance from the frame.

Samples collected along the north transect line exhibited a strong correlation between the backscatter intensity and the mean grain size (Fig. 25). The missing data are due to their location in the nadir region of the sonograph. This is the blind spot directly below the towfish. The only sample that has a very poor correlation is that at the N30 sampling point; however, the increased backscatter intensity in this region is possibly due to the larger rubble pieces, which were too large to be sampled, rather than the mean grain size. It is in these areas that the finer sands are often seen trapped between large rubble pieces. This sample was taken one year after the backscatter information was collected. This could account for the lack of correlation between the grain size and backscatter intensity at the N25 sample site. This is obvious when the 2001 samples are compared to the 2002 samples near N20. The 2001 samples correlate better to the 2001 sidescan imagery. The sands must have become mobilized between the 2001 and 2002 surveys.

The south transect line again showed a positive correlation between grain size and backscatter intensity (Fig. 26). The sand becomes more coarse as it approached the reef scarp until the last sample, which consisted of fine sands. The increased backscatter intensity in this region was most likely due to the large rubble pieces.

The east transect line displayed good correlation in both the 2001 and 2002 sediment surveys (Fig 27). The samples coarsened towards the reef scarp as the backscatter intensity increased as well.

The west transect line displayed a positive correlation between grain size and backscatter intensity (Fig 28). The best correlation in the higher backscatter portion of the line came from the 05/2001 samples. This is possibly evidence of the uncovering of

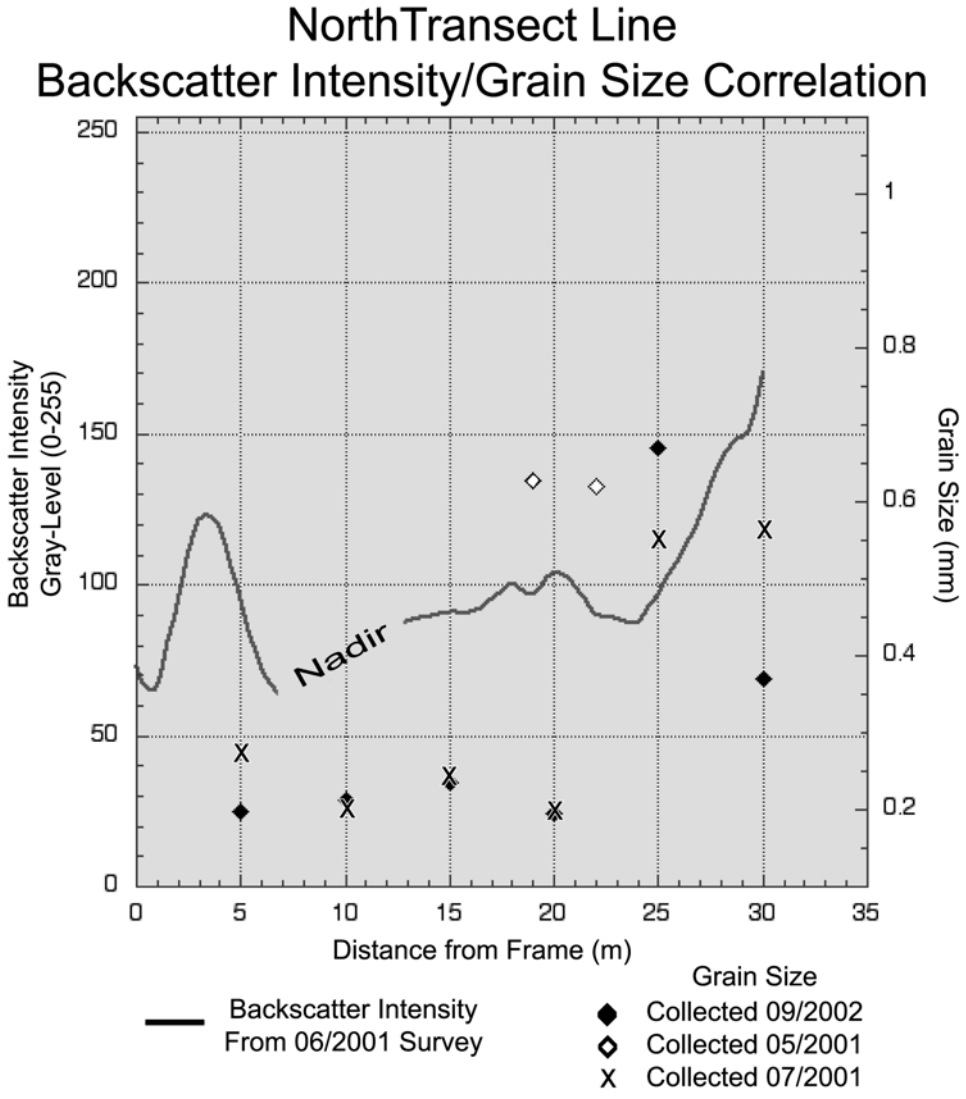

Figure 25: North transect line displaying the correlation between backscatter intensity and grain size. The grain size and backscatter intensity demonstrate a strong correlation. The missing data is due to the nadir region of the sonograph. This is the blindspot directly below the towfish. The only point that has a very poor correlation is that at the N30 sampling point, however the increased backscatter intensity in this region is possibly due to the rubble pieces rather than the sediment grain size. It is in these areas that the fine sands are often seen between large rubble pieces.

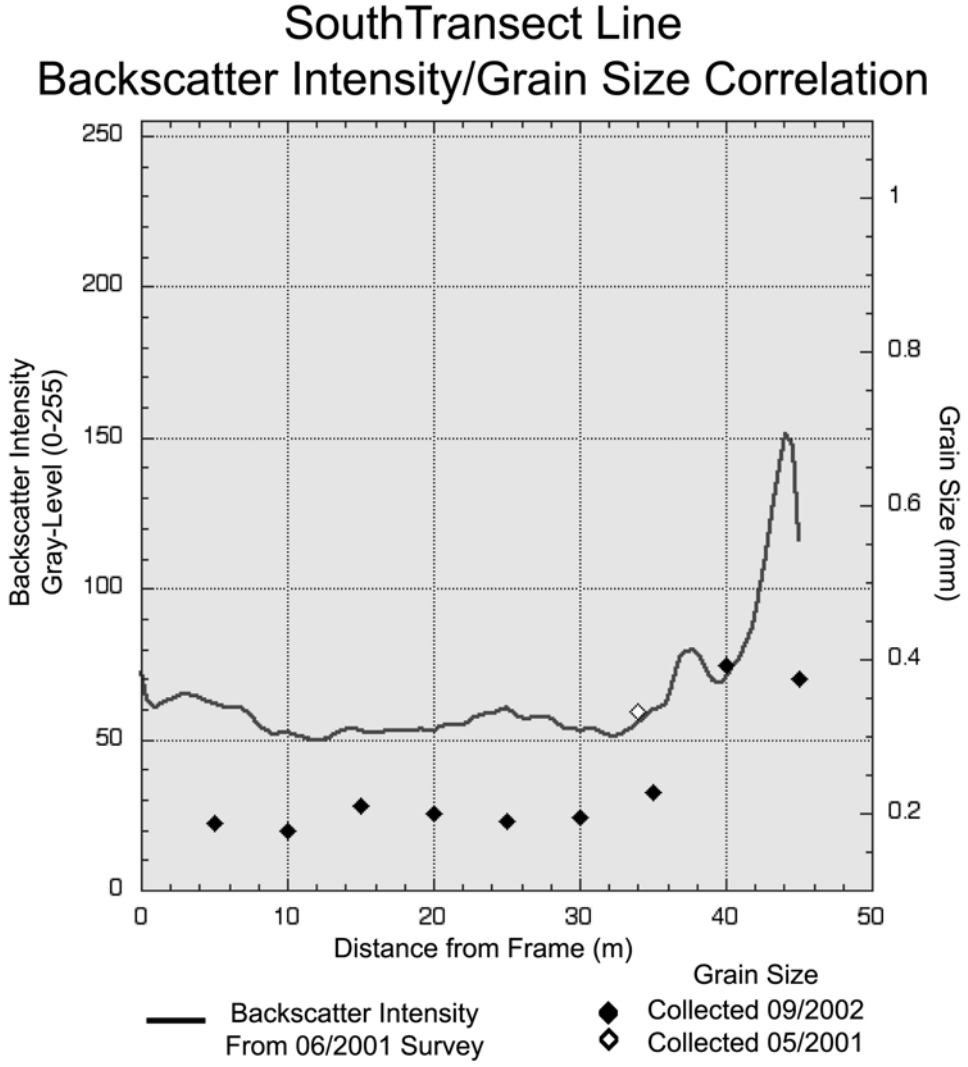

Figure 26: South transect line displaying the correlation between backscatter intensity and grain size. This graph again shows a positive correlation between grain size and backscatter. The sand coarsens as it approaches the reef scarp; however, the last sample is again fine. The increased backscatter intensity in this region is possibly due to the rubble pieces rather than the sediment grain size.

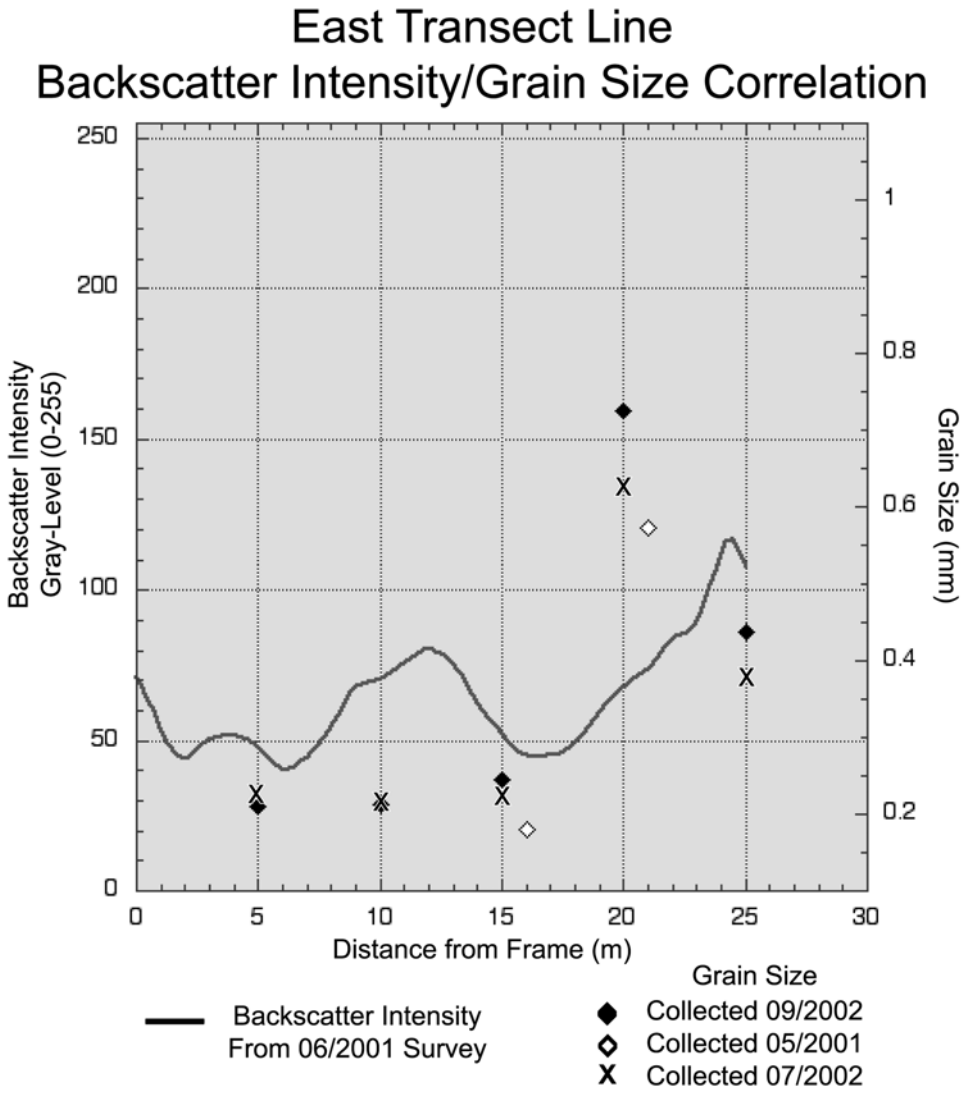

Figure 27: East transect line displaying the correlation between backscatter intensity and grain size. This graph shows good correlation in both the 2001 and 2002 sediment surveys. The samples coarsen towards the reef scarp and the backscatter intensity increases as well.

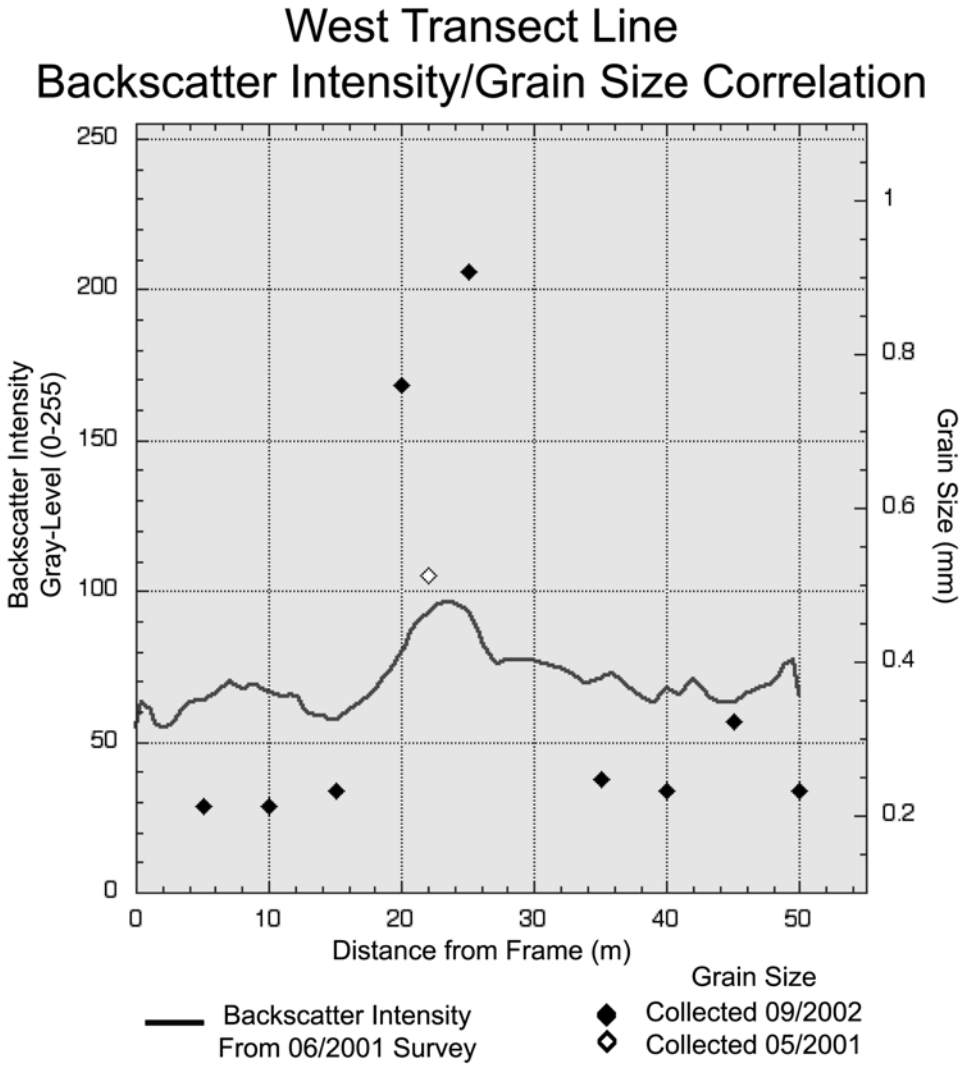

Figure 28: West transect line displaying the correlation between backscatter intensity and grain size. This graph displays a positive correlation between grain size and backscatter intensity. The best correlation in the higher backscatter portion of the line, comes from the 05/2001 sample. This is possibly evidence of the uncovering of coarser sediments in the year following the 2001 sediment samples.

coarser sediments in the year following the 2001 sediment samples, resulting in a much coarser sediment sample in 2002. The relationship of mean grain size to backscatter response was consistent throughout the transect.

The average mean grain size for the high backscatter areas was 0.63mm, and the average mean grain size for the low backscatter areas was 0.22mm. This is a bit of an underestimate for the coarse sands as the coarsest sieve was a 2mm sieve. There were many pieces far larger than that; however, this method was sufficient to differentiate between the coarse and fine sand bodies. Riggs et al., 1996 and 1998 found similar results with the coarse gravelly sands (median grain sizes=0.8-2.0) forming a lag pavement in the topographic lows between erosional scarps on the shelf floor; they do not occur on the hardbottom surfaces. Fine sands (median grain size=0.2) were found to occur as extensive thin sheets overlying the gravelly sands throughout the lower sand flats (Riggs et al., 1996, 1998).

To quantify this relationship a linear regression analysis was conducted on the data set (Fig. 29). The mean grain size was graphed against the backscatter intensity (gray level) of the sample. A linear trendline was fit to the data, and resulted in an R^2 value of 0.465. The fine samples showed a stronger correlation, while the coarser samples deviated form the trendline. This could be a result of the sediment analysis. The largest sieve size was 2mm; however, as there are grain sizes occasionally exceeding 15mm. This led to the underrepresentation of the larger grains in the mean grain size. As a result the coarser samples most likely had larger mean grain size than measured. The lack of correlation could also be a result of the shifting sands. The majority of the sediment samples were collected over a year after the sidescan data.

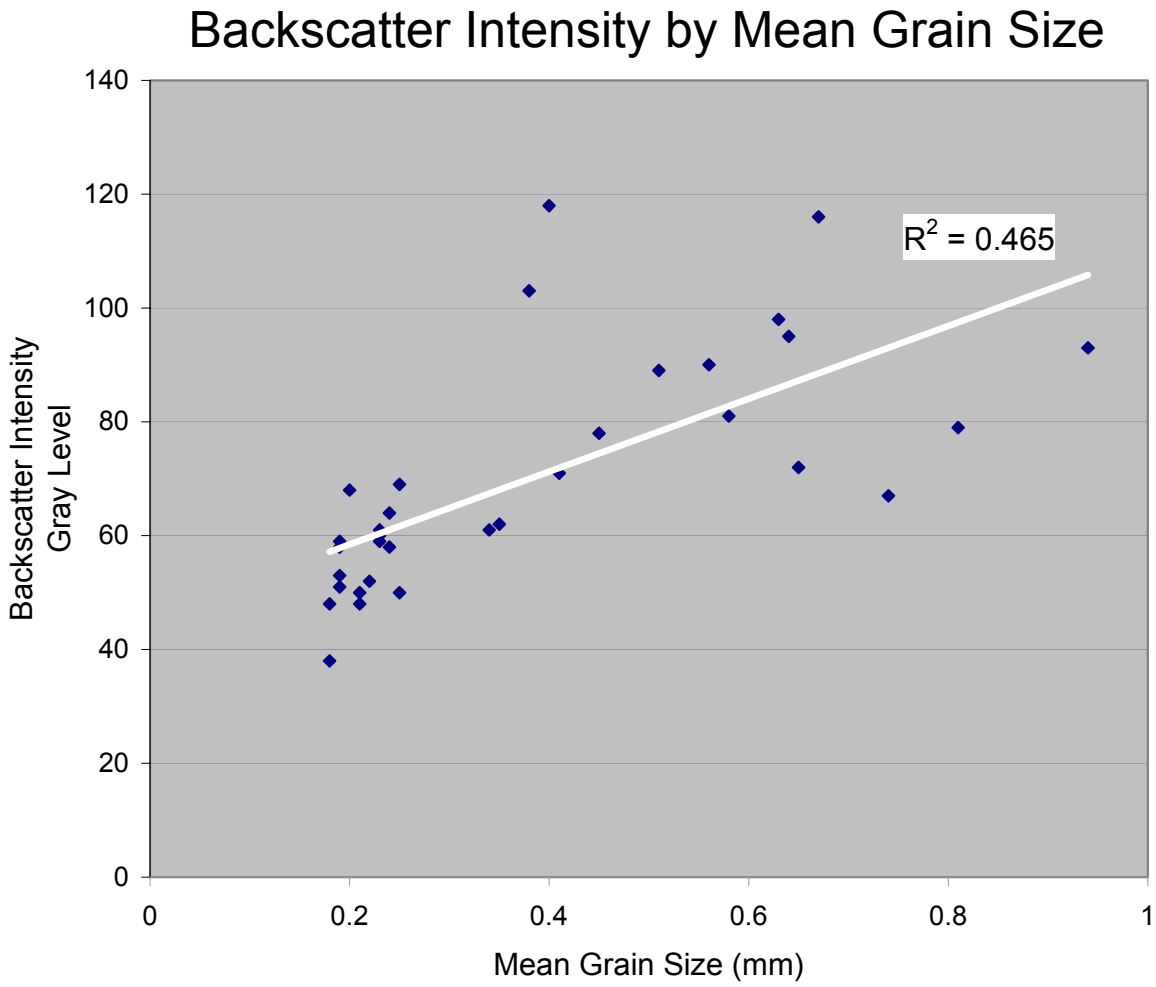

Figure 29: Linear regression analysis of the backscatter intensity (gray level) and mean grain size. The fitting of the linear trendline results in an R2 value of 0.465.

Goff et al. (2000) found a similar relationship. They found that under controlled circumstances there was a very strong correlation between grain size and backscatter intensity can be found. However, backscatter intensity is disproportionally affected by the larger grain sizes. A small increase in the percentage of the larger grain sizes (>4mm), which was typically represented by shell hash, could completely degrade the correlation (Goff et al., 2000).

A study by Davis et al. (1996) showed that backscatter intensity may increase with increasing grain size and percent carbonate composition. The backscatter returns were much higher for the coarser, higher carbonate content bodies. This is most likely not a result of the acoustic properties of $CaCO_3$, but rather more likely due to the size and shape of the carbonate particles. The shell fragments are not only typically much larger in grain size, but their shape is more acoustically significant. The shell fragments tend to have flat faces with many angles. This results in more effective scattering of acoustic energy.

Subsurface Scatterers

Ryan and Flood (1996) determined that the 100kHz sidescan sonar system is capable of detecting hard structures beneath a fine veneer of sand. These conditions are similar to those that dominate the upper hardbottom region. In many cases the Pleistocene limestone hardbottom is covered by less than 10cm of fine sands. Diver observations have revealed that in many areas the upper hardbottom looks much like the lower sand flat, as much of the surface is covered in fine sands. There are some exposed areas; however, the variability in backscatter intensity shown in the sidescan sonar

imagery is inconsistent with the relatively homogeneous surface observed by divers. It is for this reason that I believe, in most cases, the backscatter signature is a result of scattering from the underlying limestone. Subsurface scattering also may be seen in the lower sand flats. In many cases, especially near the boundaries of the fine and coarse-grained sand bodies, there is a zone of intermediate backscatter intensity. This could be due to the mobile fine sands as they begin to cover/uncover the underlying coarse sands. The 100kHz system should be capable of detecting these more intense returns of the coarse sands through a thin layer of fine sand. Therefore, the deviation in the samples from the trendline, could have been an affect of the sonar system penetrating through the finer sands and returning more intense backscatter from the underlying coarse sands. This would result in a lack of correlation between the higher backscatter of the underlying sands and the finer surficial grab samples.

Backscatter Signal of Biota

It is unlikely that the dense meadows of macroalgae observed by divers and documented in video was detected by the 100kHz sidescan system. As discussed above, the system has the ability to detect hard structures beneath a fine veneer of sand (Ryan and Flood, 1996) and, therefore, the system should be able to penetrate through the fleshy macroalgae. Evidence of this includes little to no difference in the backscatter signature adjacent to the reef scarp where dense macroalgae meadows occur and the signature of the upper hardbottom away from the reef scarp. There is also no recognizable difference in the comparisons of sonographs of various seasons (Fig. 30). Diver observations have shown a significant difference in the algal coverage of the reef edge. There is

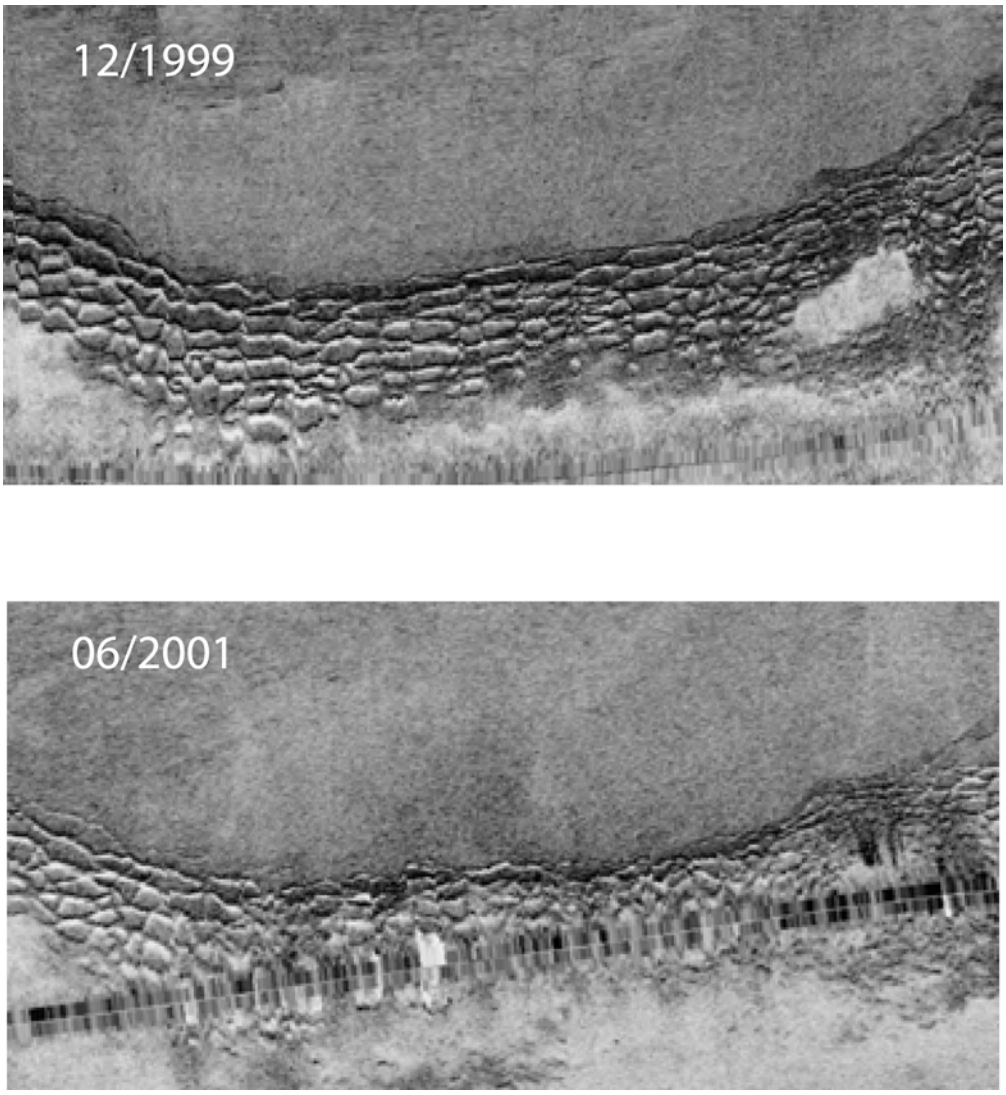

Figure 30: Seasonal comparison of the 12/1999 and 06/2001 sonographs. Diver observations have shown a significant difference in the algal coverage of the reef edge. There is significantly greater density of the macroalgae in the summer compared to the winter. However, when these sonographs are compared, there is little difference in the backscatter response. This is evidence that the 100kHz sidescan system is incapable of differentiating between the macroalgae and the reef scarp. This is most likely due to the penetration of the acoustic signal through the fleshy macroalgae, resulting in a return from the reef scarp.

significantly greater density of the macroalgae in the summer compared to the winter. However, when these sonographs are compared, there is little difference in the backscatter response. This is evidence that the 100kHz sidescan system is incapable of differentiating between the macroalgae and the reef scarp. The small dark returns on the upper hard bottom (Fig. 7b), which are depicted as 0.75-1.5m^2, are thought to be rock outcrops, sponges, and or hard corals that sit 0.25-0.50m about the seafloor. These features would all result in a high backscatter point source return and possibly produce a shadow effect in the imagery. The 500kHz system, due to its lesser degree of penetration and higher resolution, should be better suited for the detection of biota.

Seabed Classification by Textural Analysis

The three dimensional ranges for the upper hardbottom, and coarse and fines sands were used to test the feasibility of a seabed classification system. The rubble ramp values were not used as they were not distinct enough for classification purposes. A script was authored so as to classify a given pixel based upon the ranges determined by the GLCM analysis. Each pixel was classified as either *coarse*, *fine*, *upper hardbottom, or undefined*. The classification results were very promising. The coarse and fine sands were clearly identified (Fig. 31). The upper hardbottom is well defined, though there are some areas, which were classified as fine sands. This is a result of the extensive fine sand sheets on the upper hardbottom. The rubble ramp is defined as a composite of the other bottom types. The rubble ramp was found to have a range of values that intersected both the upper hardbottom values and the coarse sand values. The rubble ramp had entropy values nearly identical to the coarse sands. The homogeneity values of these

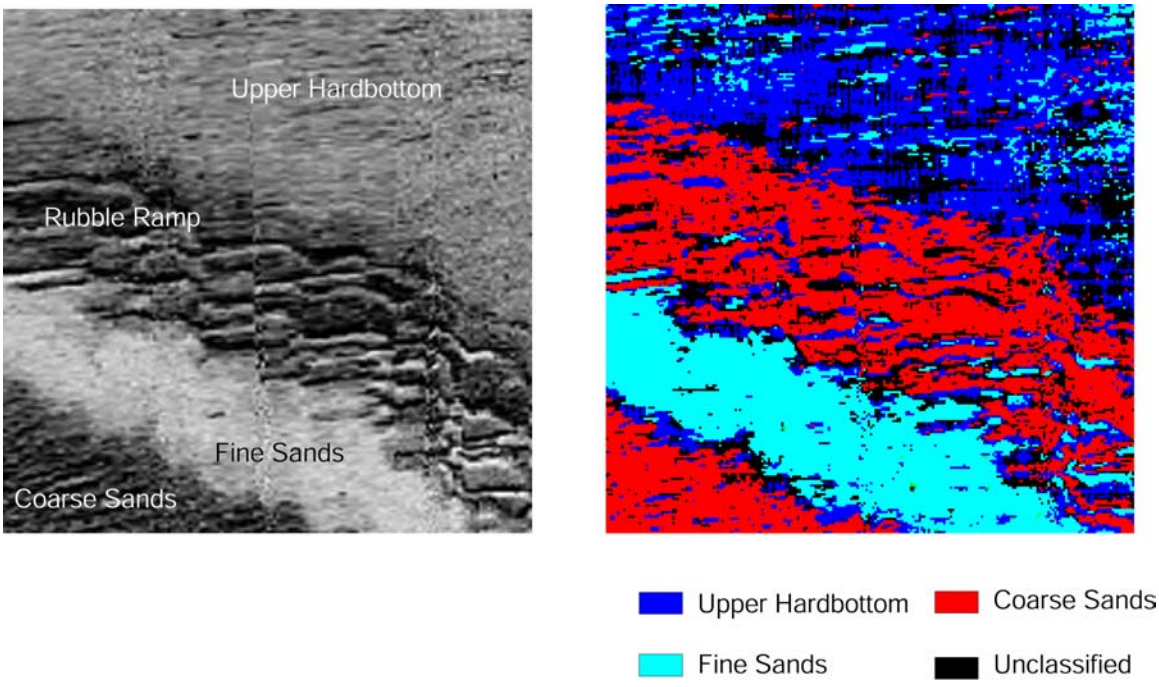

Figure 31: Textural classification of sample area of the 12/1999 sonograph. The coarse and fine sands were clearly identified. The upper hardbottom is well defined, though there are some areas, which were classified as fine sands. This is a result of the extensive fine sand sheets on the upper hardbottom. The rubble ramp is defined as a composite of the other bottom types.

seabed types were also very similar. Further refinement of the computational window, and or the use of other textural indices need to be explored before the rubble ramp can be classified with confidence. The computational window is the square area over which the center pixel is quantitatively related to other pixels across the various directional vectors of length *d.*

The GLCM classification scheme developed in this study should be adequate for seabed classification of similar geologic environments throughout Onslow Bay. The determined three-dimensional ranges for the seabed types would need calibration with groundtruthing if taken to regions with different geologic setting outside of Onslow Bay, or if acquisition or post-processing parameters were modified.

Sediment Mobilization in LSF Study Areas

A significant goal of this study was to determine how sediment properties and morphologies have changed their characteristics and spatial distribution over the 2.5 year study period.

Period 1: 12/1999 through 12/2000

The first period (1999-2000) represents an entire year of movement, which resulted in a consistent shift in the south to southeast direction in all of the areas except for LSF-4, which exhibited an easterly shift. The physical data from the moored instrument package is available from 04/27/00 through 11/30/00. This data series shows a net flux of sediments to the north-northwest (Wren, 2003). The sidescan data shows a net shift of fine-grain sands to the south-southeast. This does not fit the physical data; however, the physical data do not include 12/99-04/26/00. It is this time of year that is

often dominated by northern wind events (nor'easters). These northern wind events have been shown to produce near-bottom currents in a southerly direction (Wren, 2003).

Wren (2003) observed a spring nor'easter that passed by the study site 05/29/00-06/01/00. Preceding the event, moderate southeasterly winds were dominant before suddenly switching around out of the north on 05/29. Once the wind switch occurred, wave heights increased to 1.5-2.0m and greater for 48 hours. Observed near-bottom orbital velocities ranged from 20-30cms^{-1} at 1m above the bed (1mab). The mean current data from the PCADP shows a 24hr lag in the near-bottom flow response to the wind switch. The flows switched from northerly to south-southeasterly. Suspended sediment transport during this event was evident in the signal amplitude collected from the OBS sensors. The seabed altimetry data suggest that bedload transport occurred, as changes of 1-2cm in relief are apparent.

A southern near-bottom current was also observed by Wren (2003) during a nor'easter that occurred at the site from 09/06/00 to 09/08/00. Preceding the event, conditions were typical of fair weather conditions (winds < 10ms^{-1} and waves < 1m), which were dominant for several days before suddenly switching to the northeast on 09/06/00 (Wren and Leonard, 2003). Significant wave heights increased to 2.0-3.0m for 48 hours. Wave periods were 5 to 8 seconds and were comparable to the wave periods that were observed during the 05/29/00-06/01/00 nor'easter. Observed near-bottom orbital velocities ranged from 25-35cms^{-1} at 1mab. These currents were directed to the southwest. The seabed altimeter recorded erosion of 3cm during the first 24hrs of the event, suggesting sediment mobility.

Period 2: 12/2000 through 06/2001

This period comprised the winter and spring seasons. The movement observed in the sidescan displayed a consistent shift to the north-northwest in all study areas except LSF-4, which shifted to the west; and LSF-1, which shifted to the northeast. The shifts in the contacts of the fine/coarse-grained sand bodies could be a result of the seasonal weather patterns in the winter and spring.

Physical data collected 04/27/00-05/31/00, 03/01/01-03/31/01, and 12/01/01-02/28/02, display an apparent suspended sediment flux at 1mab in the north-northwest direction (Wren, 2003). There are several mechanisms capable of shifting fine sands in this direction. The first mechanism could be a southerly wind event (Wren, 2003), as in the case of the 11/25/2000 to 11/28/2000 event. Preceding this event winds were typical of this time of year with moderate northerly winds. On 11/25 the winds switched to a southeasterly and later southwesterly direction with velocities ranging from 16-21ms^{-1}. The large fetch resulted in waves of 4-5m with periods of 9-10s. Observed orbital velocities were ~25cms^{-1} at 1mab. Near bottom currents were dampened by the semi-diurnal tidal signal; however, accretion of ~2cm occurred during this event. The OBS sensors marked an immediate increase in the suspended sediments that remained for 48hrs.

Aside from wind and storm events, fair-weather events appear to have a significant effect on the sediment mobility at this site (Wren, 2003). This fair-weather event took place 06/02/00 through 06/27/00. The waves during this period were < 1m and near-bottom tidal flows were ~10cms^{-1}. While this mechanism along does not result in significant sediment mobilization (Wren, 2003), a Gulf Stream intrusion also occurred

during this time. The intrusion of this current resulted in subtidal flows to the north. This resulted in sediment mobilization and significant accretion at the framesite (Wren, 2003).

Near Reef Sites: LSF-1 & LSF-4

In looking at the sand displacements it is obvious that the LSF-1 and LSF-4 sample areas differ in displacement magnitude and direction when compared to the other subareas. Since the reef ledge contains numerous features that may be used as geographical benchmarks, there is greater confidence in the accuracy of the calculated displacements of high/low backscatter boundaries. The results are therefore not directly attributed to navigation error. Once possible factor is the proximity of these sites to the reef and associated hydrodynamic conditions. The reef itself could affect the mobility of the adjacent sediments by changing the near bottom current magnitudes and direction.

The 1999-2000 surveys exhibited significant displacement to the east (LSF-4) and southeast (LSF-1). This time period also marked significant changes in the morphology of the high/low backscatter boundaries for the LSF-4 area. The 2000-2001 period revealed no significant movement at LSF-1, but showed a significant displacement to the west at LSF-4. There was little morphological change from 2000-2001 in either of the areas. There was significant displacement and morphological change in an eastern direction from 1999-2001 at both sites. These sites exhibited similar patterns in both direction and magnitude over the length of the study with some differentiation from 2000-2001. It appears that the two sites, though separated by 850m, were subject to similar oceanographic conditions. There is some concern in the association of the surface conditions and near-bottom conditions, as the reef scarp appears to affect the near bottom

currents. This is evident in looking at the ADCP vs. PCADP data for 12/01/01 through 02/28/02. The ADCP data measures the upper water column (above the reef scarp), and the PCADP measures the near bottom current profile. The ADCP data for this period indicates a net flow to the southwest, while the PCADP data observed a net flow to the north. It is for these reasons that the near-reef sites may not exhibit the same direction and magnitude displacements as the far-reef sites.

CONCLUSIONS

High-resolution sidescan sonar has been used to map and monitor a hardbottom area on the mid-continental shelf of Onslow Bay over a 2.5 year period. Analysis of these data, together with diver observations, sediment sampling and physical measurements collected during the same time period, can be used to draw the following conclusions:

- At the study site, higher backscatter areas are composed of largely heterogeneous and poorly sorted sediments with relatively large grain size and relatively high carbonate content. Low backscatter areas are associated with homogenous, well-sorted fine sand bodies. This direct relationship between backscatter intensity and grain size agrees with previous studies (e.g. Ryan and Flood, 1996; Goff 1999, 2000; LeBlanc et al., 1995; Davis et al., 1996) that were conducted at a much larger scale and lower resolution. Subsurface scattering also appears to play a role in backscatter intensity, particularly in the upper hardbottom area where it is

believed the sonar is able to penetrate the thin (<10 cm) veneer of fine-grain sediments overlying Pleistocene limestone. It is possible that sessile organisms (corals, sponges) on the upper hardbottom that extend up to 0.25-0.50 cm above the seafloor are imaged by the sonar system. It is unlikely, however, that the dense meadows of macroalgae are resolvable. The system has the ability to detect hard structures beneath a fine veneer of sand (Ryan and Flood, 1996) so, the system should be able to penetrate through the fleshy macroalgae. This becomes evident as there is little to no difference in the backscatter signature adjacent to the reef scarp where dense macroalgae meadows are observed, and the signature of the upper hardbottom away from the reef scarp.

- The gray-level co-occurrence analysis proved to be an effective tool in quantitatively identifying seabed types in sidescan sonar imagery. Using the textural indices entropy and homogeneity, coupled with gray-level values, three of the four seabed types were identified: upper hard bottom, fine-grain sand bodies and coarse-grain sand bodies. Due to overlapping ranges we were unable to identify the rubble ramp with confidence. The preliminary classification proved effective in identifying the upper hardbottom, and coarse and fine sands. Further refinement of this method, including changing computational window sizes and incorporation into a classification module to allow automatic classification of large areas, is planned.
- Four repeat sidescan surveys were used to document displacements in fine-coarse grain sand body contacts. Significant displacements (>10m) and changes in morphology of contacts in five study areas suggest that the fine-grain sands in this

area are highly mobile. The first observation period (1999-2000) represents an entire year of movement, which resulted in a consistent shift in the south to southeast direction in all of the areas except for one. The second observation period (2000-2001) comprised the winter and spring seasons. The contact movement displayed a consistent shift to the north-northwest in all study areas except two. Seasonal variations were noted in the physical data, as the spring and summer exhibited currents to the southwest in the along shelf direction and currents towards the shore (northwest) in the across shelf direction. The fall and winter exhibited currents to the northeast in the along shelf direction and offshore currents (southeast) in the across shelf direction. Individual events (nor'easters and fair-weather) recorded in the physical data provide mechanisms for the observed sand movement seen in the sidescan surveys. Anomalous results for two sites near the reef suggest hydrodynamic influences brought about by the seafloor relief associated with the reef.

REFERENCES

Blondel, P., Sempere, J.C., Robigou, V. 1993. Textural analysis and structure tracking for geological mapping: applications to sonar images from Endeavour segment, Juan de Fuca Ridge. *Oceans '93 IEEE* 3/93, p. 208-213

Blondel, P. and Murton, B.J.1997. Handbook of Seafloor Sonar Imagery. John Wiley and Sons: Chichester, UK.

Blondel, P., et al. 1998. TexAn: Textural analysis of sidescan sonar imagery and generic seafloor characteristics. *IEEE* 6/98, p. 419-423.

Brown, C.J., Cooper, K.M., Meadows, W.J., Limpenny, D.S., and Rees, H.L. 2002. Small-scale mapping of sea-bed assemblages in the Eastern English Channel using sidescan sonar and remote sampling techniques. *Estuarine, Coastal, and Shelf Science*, v. 54, p. 263-278.

Chavez Jr., P.S., Isbrecht, J., Galanis, P., Gabel, G.L., Sides, S.C., Soltesz, D.L., Ross, S.L., Velasco, M.G. 2002. Processing, mosaicking, and management of the Monterey Bay digital sidescan-sonar images. *Marine Geology*, v. 181, p. 305-315.

Chotiros, N.P., Altenburg, R., and Piper, J. 1997. Analysis of acoustic backscatter in the vicinity of the Dry Tortugas. *Geo-Marine Letters*, v. 17, p. 325-334.

Cochrane, G.R., and Lafferty, K.D. 2002. Use of acoustic classification of sidescan sonar data for mapping benthic habitat in the Northern Channel Islands, California. *Continental Shelf Research*, v. 22, p. 683-690.

Davis, K.S., Slowey, N.C., Stender, I.H., Fiedler, H., Bryant, W.R., and Fechner, G. 1996. Acoustic backscatter and sediment textural properties of inner shelf sands, northeastern Gulf of Mexico. Geo-Marine Letters, v. 16, p. 273-278.

Folk, R.L., 1974. The Petrology of Sedimentary Rocks: Hemphill Publishing Co.: Austin, TX, pp. 182.

Gao, D., Hurst, S.D., Karson, J.A., Delaney, J.R., and Spiess, F.N.1998. Computer-aided interpretation of side-looking sonar images from the eastern intersection of the Mid-Atlantic ridge with Kane Transform. *Journal of Geophysical Research*, v. 103, n. B9, p. 20,997-21,014.

Goff, J.A., Swift, D.J.P., Duncan, C.S., Mayer, L.A., Hughes-Clark, J. 1999b. High-resolution swath sonar investigation of sand ridge, dune and ribbon morphology in the offshore environment of the New Jersey margin. *Marine Geology*, v. 161, p. 307-337.

Goff, J.A., Olson, H.C., and Duncan,C.S.2000. Correlation of side-scan backscatter intensity with grain-size distribution of shelf sediments, New Jersey margin. *Geo-Marine Letters,* v. 20, p. 43-49.

Haralick, Robert M. 1979. Statistical and structural approaches to texture. *IEEE* v. 67, n. 5, p. 786-804.

Johnson, P.J., & Helferty, M. 1990. The geological interpretation of side-scan sonar. *Reviews of Geophysics*, v. 28, p. 357-380.

LeBlanc, L.R., Satchidanan, P., and Schock, S.G. 1992. Sonar attenuation modeling for classification of marine sediments. *Journal of the Acoustical Society of America*, v. 91 n. 1, p. 116-126.

LeBlanc, L.R., Schock, S.G., DeBruin, D.L., and Jenkins, M. 1995. High-resolution sonar volume scattering measurements in marine sediments. *Journal of the Acoustical Society of America*, v. 97, n. 5, p. 2979-2986.

Ojeda, G.Y, Gayes, P.T., Van Dolah, R.F., and Schwab, W.C. 2004. Spatially quantitative seafloor habitat mapping: example from the northern South Carolina inner continental shelf. *Estuarine, Coastal and Shelf Science,* in press.

Posey, M.H. and W.G. Ambrose, Jr. 1994. Effects of proximity to an offshore hard-bottom reef on infaunal abundances. *Marine Biology* 118: 745-753.

Posey, M., W. Lindberg, T. Alphin and F. Vose. 1996. Influence of storm disturbance on an offshore benthic community. Bulletin of Marine Science 59: 523-529.

Renaud, P.E., W.G. Ambrose, Jr., S.R. Riggs and D.A. Syster. 1996. Multi-level effects of severe storms on an offshore temperate reef system: Benthic sediments, macroalgae, and implications for fisheries. *Marine Ecology* 17: 383-398.

Renaud, P.E., S.R. Riggs, W.G. Ambrose, Jr., K. Schmid and S.W. Snyder. 1997. Biological-geological interactions: Storm effects on macroalgal communities mediated by sediment characteristics and distribution. *Continental Shelf Research* , v. 17, p. 37-56.

Riggs, S., Snyder, S.W., Hine, A.C. and Mearns D.L., 1996. Hardbottom morphology and relationship to the geologic framework: Mid-Atlantic continental shelf, *Journal of Sedimentary Research*, v. 66, p. 830-846.

Riggs, S.R., W.G. Ambrose, Jr. J.W. Cook, S.W. Snyder and S.W. Snyder. 1998. Sediment production on sediment-starved continental shelf margins: The interrelationship between hard bottoms, sedimentological and benthic community processes, and storm dynamics. Journal of Sedimentary Research Section A: *Sedimentary Petrology*, v. 68, p. 155-148.

Ryan, W.B.F., & Flood R.D 1996. Side-looking sonar backscatter response at dual frequencies. *Marine Geophysical Researches*, v. 18, p. 689-705.

Shokr, Mohammed E. 1991. Evaluation of second-order texture parameters for sea ice classification from radar images. *Journal of Geophysical Reasearch*, v.96, n. C6, p10625-10640.

Tso, B.,and Mather, P.M. 2001. Classification Methods for remotely Sensed Data. Taylor and Francis Inc., New York, NY.

Wren, A., 2004. Sediment Transport Adjacent to a Marine Hardbottom on the Mid-Continental Shelf: Onslow Bay, NC. Unpublished doctoral dissertation. Submitted to North Carolina State University.

APPENDICES

Appendix A: Geometric and radiometric correction parameters

Corrections/Enhancements within Triton Elic's ISIS Module

1. Time Varying Gain (TVG) and Balance (This is used to balance the returns across track as the signal is increasingly attenuated)
    a. Channel = All
    b. Custom settings used starting at transmit
    c. DC Offset = +0.00V
    d. Balance = On
    e. Channel-to-channel = On
    f. Darkness = 4% Max
    g. Decay Rate = 26
2. Bottom Track (for slant range correction)
    a. Method = Manual
    b. Channel = 1
    c. Level = Data dependent(This value ranged from 7%-35%)
    d. Holdoff = Data dependent(This value should be held as close to the actual depth as possible, as it removes the thermocline and other reflectors within the water column)
3. DelphMosaic and DTM
    a. Map and Projection Settings
        i. Resolution = 0.25m
        ii. Depth = <2000m

iii. Units = dd.dddd

iv. Output Projection = Universal Transverse Mercator

v. Datum = WGS Datum (1984)

b. Use Nav from Coverage Map = On

c. Apply Layback to Nav in Mosaic = On

i. Setup = Compute layback from cable out

1. Cable out = Survey dependent (27-30m)

d. For sensor direction use = Course made good

e. Fill gaps between pings = On

f. Merge overlapping lines by = Cover up

1. Corrections/Enhancements within Triton Elics' DelphMap Module. Define Palettes

a. Data Type = Sidescan

b. Palette = Gray

c. Palette Density = Logarithmic(Linear stretching of the gray scale resulting in the best contrast for our applications)

d. Reverse = On(Reverses gray values from standard convention, resulting in the more intense returns being the darker returns)

Import into ARCVIEW:

This was done through manipulating the *.tfw file. This is the georefrencing header that accompanies the *.tif file. This header consists of the upper left hand corner

coordinates of the image file and the resolution. Changing this reference file essentially moves the mosaic in space until all of the fixed points in each mosaic line up. This allowed for a more accurate analysis of the temporal changes of sediment boundaries in the successive mosaics.

Appendix B: Gray level co-occurrence matrices analysis using "t_co_occurrence.exe" (an algorithm authored by Brandt Tso) in the Cygwin interface.

1. Gray level data from the 96 x 96 pixel sample area must be converted to ASCII format. In the Graphic Converter software A 96 x 96 pixel image is cut from the appropriate seabed type in the *.tif file. This is then saved in ASCII format.
2. This is then processed by the glcm executable using the following parameters

```
$ ./glcm.exe
Please input the number of image rows:96
Please input the number of image columns:96
Please input the window size (3, or 5, or 7,): 19
Please input the value for d:15 (d=vector length along which,
pixels are quantitatively related to the central pixel)
Please input the value of gray levels:256
Please input image for proccessing:Rubble.txt
```

This will result in 5 files being created: Angular Second Moment, Entropy, Inverse Difference Moment (homogeneity), Contrast, and Correlation. The two applicable files will be the "entropy" and "idm" files. The "idm" file is the homogeneity file. These files will be 87 x 87 pixels in area and must be converted to single columns. These files are then imported into a spreadsheet program and arranged into 3 columns using the gray level values from the initial ASCII file as the other column. The gray level

values must first be converted from a 96 x 96 pixel area to a 87 x 87 pixel area to match the entropy and idm files. The gray level values are then converted to a single column. These columns will represent the xyz axes in the three dimensional display of the values. The entropy file will be in the x column, the gray level will be in the y column, and the homogeneity file will be the z column. This is then saved as a tab delimited *.txt file.

Appendix C: Graphing the entropy, homogeneity, and gray level in three dimensions.

The graphing is done by the "psxyz" three-dimensional graphing module found in the Generic Mapping Tools software package. The following script is used to graph two separate xyz files (input_file#1.txt and input_file#2.txt) on the same graph:

```
gmtset PAPER_MEDIA letter+

psxyz -JX12/12l -JZ9 -R2.4/3.2/.01/1/0/255 -
Ba.2f.20/a10f3p/a50f50:."":WeSnZ -Sc0.03-Dglcmplot1 -
G0/255/0 -E200/30 input_file#1.txt -V -P -K >
output_file.ps
```

psxyz -JX12/12l -JZ9 -R2.4/3.2/.01/1/0/255 -Sc0.01 -G0/0/255 -E200/30 input_file#2.txt -V -O >> output_file.ps

This results in the postscript file "output_file.ps".

More information can be found by using the command: "man psxyz"

Figure 3: Trackline map for repeat surveys at 23 Mile site superimposed on NGDC coastal relief model gridded at a 3 arc second interval. Bathymetric contour interval is 1 m. Lines are 3.5nm long and spaced 200 m apart.

Figure 6: Seabed map of 23 Mile site showing the four distinct bottom types: upper hardbottom, rubble ramp, coarse sands, and fine sands. This map is based on the 12/1999 sidescan mosaic, diver observations, and sediment sampling.